

Convergence of first-order Finite Volume Method based on Exact Riemann Solver for the Complete Compressible Euler Equations

Mária Lukáčová-Medviďová, Yuhuan Yuan

*Institute of Mathematics, Johannes Gutenberg-University Mainz
Staudingerweg 9, 55128 Mainz, Germany*

Abstract

Recently developed concept of dissipative measure-valued solution for compressible flows is a suitable tool to describe oscillations and singularities possibly developed in solutions of multidimensional Euler equations. In this paper we study the convergence of the first-order finite volume method based on the exact Riemann solver for the complete compressible Euler equations. Specifically, we derive entropy inequality and prove the consistency of numerical method. Passing to the limit, we show the weak and strong convergence of numerical solutions and identify their limit. The numerical results presented for the spiral, Kelvin-Helmholtz and the Richtmyer-Meshkov problem are consistent with our theoretical analysis.

Keywords: compressible Euler equations, finite volume method, exact Riemann solver, dissipative measure-valued solution, convergence

1. Introduction

Hyperbolic conservation laws play an important role in describing many physical and engineering process. An iconic example is the nonlinear system of compressible Euler equations, which governs the dynamics of a compressible material and incorporates mass, momentum and energy conservation.

A characteristic feature of nonlinear conservation laws is that discontinuities (shock waves) may develop after finite time even if the initial condition is smooth. A natural way to overcome this difficulty would be to work with a concept of weak distributional solution. However, it is well-known that such weak solutions fail to be unique. Consequently, the second law of thermodynamics have been proposed as a selection criterion to rule out nonphysical solutions. The entropy production principle have been successfully applied in the scalar multidimensional equations [27] and one-dimensional systems [3, 4].

Email addresses: lukacova@uni-mainz.de (Mária Lukáčová-Medviďová), yuhuyuan@uni-mainz.de (Yuhuan Yuan)

Unfortunately, it completely fails for multidimensional systems. Recently, De Lellis and Székelyhidi [8] and Chiodaroli et al. [7] showed non-uniqueness of weak entropy solutions for the multidimensional isentropic compressible Euler system, see also [8] for similar non-uniqueness results for the incompressible Euler system. These results have been extended to the complete Euler system in Feireisl et al. [13].

In order to describe oscillations arising in the limits of singular perturbations of hyperbolic conservation laws, a more generalized solution, i.e. measure-valued (MV) solution, was suggested by DiPerna. In 1985 he showed for one-dimensional hyperbolic conservation laws that regularized solutions of associated diffusive and dispersive regularized systems converge to a MV solution, as a regularized parameter vanishes [10]. Recently the concept of MV solution was adapted and applied for multidimensional compressible Euler system [26] and three-dimensional incompressible Euler equations [11], see also [2, 28].

In this paper we work with the concept of *dissipative measure-valued (DMV) solution* for the complete Euler system, which enjoys the weak-strong uniqueness principle [5]. Analogous concept has been adopted for the isentropic Euler system [23], compressible Navier-Stokes system [12], elastodynamics [9] and other related problems.

In the convergence analysis of numerical schemes for hyperbolic conservation laws the entropy stability plays a crucial role, we refer a reader to a seminal paper of Tadmor [29]. For multidimensional hyperbolic conservation laws the convergence analysis to MV solutions was studied by Fjordholm et al. [22, 21]. For the Lax-Friedrichs and vanishing viscosity finite volume method, Feireisl, Lukáčová and Mizerová generalized the above convergence result for the Euler system and proved the convergence to the DMV solution and the classical solution on its lifespan [15, 14]. For generalization to viscous compressible flows we refer a reader to [17, 18]. In [16, 19] a new tool, \mathcal{K} -convergence, has been developed to compute strong limits of oscillatory sequences of numerical solutions.

In the present paper we focus on the first-order finite volume method based on the exact Riemann problem solver for the complete compressible Euler system and show its convergence via the concept of DMV solutions. We will only assume that our numerical solutions stay in a physically non-degenerate region, i.e. density is bounded from below and energy is bounded from above. Interestingly, this assumption is equivalent to the strict convexity of the mathematical entropy, see Lemma B.4.

The rest of the paper is organized as follows. In Section 2 we introduce suitable notations and describe the finite volume method with a numerical flux based on the exact solution of the local Riemann problem, cf. Godunov method. In Section 3 we analyze the entropy inequality and give an explicit lower bound of the entropy Hessian matrix, see Appendix B. A crucial step is to show the consistency of our numerical method. Section 4 is devoted to the limiting process. We prove that the numerical solutions will generate a weakly-(*) convergent subsequence and a Young measure, a DMV solution, to the Euler system. Furthermore, employing the theory of \mathcal{K} -convergence and DMV-strong uniqueness principle, we obtain the strong convergence of the Cesàro averages and strong convergence of numerical solutions to the weak/strong/classical solution. Finally,

in Section 5 we present numerical simulations and illustrate the effects of \mathcal{K} -convergence of numerical solutions. The numerical results clearly demonstrate convergence results being consistent with our analysis. As far as we know this is the first result in literature where the convergence of a well-known Godunov method has been proved rigorously for multidimensional Euler equations.

2. Numerical method

The complete Euler system can be written in the divergence form

$$\partial_t \mathbf{U} + \operatorname{div}_{\mathbf{x}} \mathbf{F}(\mathbf{U}) = 0, \quad (t, \mathbf{x}) \in (0, T) \times \Omega, \quad (2.1)$$

where \mathbf{U}, \mathbf{F} denote the conservative vector and flux, defined by

$$\mathbf{U} = (\rho, \mathbf{m}, E)^T, \quad \mathbf{F}_i(\mathbf{U}) = (\rho u_i, u_i \mathbf{m} + p \mathbf{e}_i, u_i(E + p))^T, \quad i = 1, \dots, d.$$

Here ρ denotes density, $\mathbf{u} := (u_1, \dots, u_d)$ velocity, $\mathbf{m} := \rho \mathbf{u}$ momentum, $E := \frac{\rho |\mathbf{u}|^2}{2} + \rho e$ total energy, p pressure, e internal energy, and the row vector \mathbf{e}_i represents the i -th row of the unit matrix of size $d := \dim(\mathbf{x}), d = 1, 2, 3$.

Throughout the whole text, we consider the bounded domain $\Omega \subset \mathbb{R}^d$ together with the space-periodic or no-flux boundary condition. Moreover, the equation of state is restricted to

$$p = (\gamma - 1)\rho e, \quad (2.2)$$

where $\gamma \in (1, 2]$ is the adiabatic constant.

Remark 2.1. For the Euler system (2.1) the mathematical entropy pair can be given by

$$\eta = \frac{-\rho S}{\gamma - 1}, \quad \mathbf{q} = \frac{-\rho S \mathbf{u}}{\gamma - 1} = \eta \mathbf{u} \quad (2.3)$$

with thermodynamic entropy S defined by

$$S := \ln(p) - \gamma \ln(\rho). \quad (2.4)$$

The corresponding entropy variable and entropy potential are given by

$$\boldsymbol{\nu} := \nabla_{\mathbf{U}} \eta = \begin{pmatrix} \frac{\gamma - S}{\gamma - 1} - \frac{\rho |\mathbf{u}|^2}{2p} \\ \frac{\rho \mathbf{u}}{p} \\ -\frac{\rho}{p} \end{pmatrix}, \quad \psi = \rho \mathbf{u}, \quad (2.5)$$

respectively. We require that in addition to (2.1) the entropy inequality holds, i.e.

$$\partial_t \eta(\mathbf{U}) + \operatorname{div}_{\mathbf{x}} \mathbf{q}(\mathbf{U}) \leq 0. \quad (2.6)$$

2.1. Spatial discretization and notations

The computational domain Ω consists of rectangular meshes $\bar{\Omega} := \bigcup_K \bar{K}$. We denote the set of all mesh cells as \mathcal{T}_h , σ stands for cell face, a unit normal vector to σ is \mathbf{n} , the face between two neighboring cells K and L is denoted by $\sigma_{K,L} = K|L$, and the set of all interior faces is given as $\Sigma_{\text{int}} = \{\sigma \in \Sigma : \sigma \cap \partial\Omega = \emptyset\}$. Moreover, for $\mathbf{x} \in \sigma$ we define

$$a^{\text{out}}(\mathbf{x}) = \lim_{\delta \rightarrow 0^+} a(\mathbf{x} + \delta \mathbf{n}), \quad a^{\text{in}}(\mathbf{x}) = \lim_{\delta \rightarrow 0^+} a(\mathbf{x} - \delta \mathbf{n}) \quad (2.7)$$

and introduce the standard average- and jump-operators

$$\{a\} = \frac{a^{\text{in}} + a^{\text{out}}}{2}, \quad [[a]] = a^{\text{out}} - a^{\text{in}}. \quad (2.8)$$

We use the notation $a \lesssim b$ if there exists a generic constant $C > 0$ independent on the mesh discretization, such that $a \leq C \cdot b$ for $a, b \in \mathbb{R}$.

2.2. Discrete function space and finite volume method

Consider the space of piecewise constant functions

$$\mathcal{Q}_h(\Omega) = \{v : v|_{K^\circ} = \text{constant, for all } K \in \mathcal{T}_h\}. \quad (2.9)$$

We can define the projection

$$\Pi_h : L^1(\Omega) \rightarrow \mathcal{Q}_h(\Omega), \quad \Pi_h[\phi]_K = \frac{1}{|K|} \int_K \phi(x) dx, \quad (2.10)$$

where $|K|$ is the Lebesgue measure of K .

Let $\mathbf{U}_h \in \mathcal{Q}_h(\Omega; \mathbb{R}^{d+2})$. We consider a semi-discrete finite volume method

$$\frac{d}{dt} \mathbf{U}_K(t) + (\text{div}_h \mathbf{F}_h(t))_K = 0, \quad t > 0, \quad K \in \mathcal{T}_h, \quad (2.11a)$$

$$\mathbf{U}_K(0) = \Pi_h(\mathbf{U}^0)_K, \quad K \in \mathcal{T}_h, \quad (2.11b)$$

where the numerical flux function \mathbf{F}_h is given by means of the exact Riemann solver [30]. Consequently, (2.11a) can be rewritten as

$$\int_K \frac{d}{dt} \mathbf{U}_K(t) d\mathbf{x} + \sum_{\partial K \cap \partial L \neq \emptyset} \int_{\partial K \cap \partial L} \mathbf{F}(\mathbf{U}_{\sigma_{K,L}}^{RP}) \cdot \mathbf{n}_K dS_{\mathbf{x}} = 0, \quad (2.12)$$

where $\mathbf{U}_{\sigma_{K,L}}^{RP}$ is the solution of a local Riemann problem at face $\sigma_{K,L}$. A piecewise constant solution $\mathbf{U}_h = \{\mathbf{U}_K; K \in \mathcal{T}_h\}$ satisfies an equivalent weak form

$$\int_{\Omega} \phi \frac{d}{dt} \mathbf{U}_h d\mathbf{x} - \sum_{\sigma \in \Sigma_{\text{int}}} \int_{\sigma} \mathbf{F}(\mathbf{U}_{\sigma}^{RP}) \cdot \mathbf{n} [[\phi]] dS_{\mathbf{x}} = 0, \quad (2.13)$$

where $\phi \in \mathcal{Q}_h(\Omega)$.

Remark 2.2. From here on, we write $(x, y)^T$ rather than \mathbf{x} for $d = 2$, and $(x, y, z)^T$ for $d = 3$. For a two-dimensional uniform mesh a general cell is denoted by $K_{ij} = (x_{i-\frac{1}{2}}, x_{i+\frac{1}{2}}) \times (y_{j-\frac{1}{2}}, y_{j+\frac{1}{2}})$ with (x_i, y_j) as the center, $\Delta x = x_{i+\frac{1}{2}} - x_{i-\frac{1}{2}}$ and $\Delta y = y_{j+\frac{1}{2}} - y_{j-\frac{1}{2}}$. Hence, (2.12) can be rewritten as

$$\frac{d}{dt} \mathbf{U}_{ij}(t) + \frac{1}{\Delta x} \left(\mathbf{F}_1(\mathbf{U}_{i+\frac{1}{2},j}^{RP}) - \mathbf{F}_1(\mathbf{U}_{i-\frac{1}{2},j}^{RP}) \right) + \frac{1}{\Delta y} \left(\mathbf{F}_2(\mathbf{U}_{i,j+\frac{1}{2}}^{RP}) - \mathbf{F}_2(\mathbf{U}_{i,j-\frac{1}{2}}^{RP}) \right) = 0,$$

where $\mathbf{U}_{ij} := \mathbf{U}_{K_{ij}}$ and $\mathbf{U}_{i+\frac{1}{2},j}^{RP}$ is the solution at $(x_{i+\frac{1}{2}}, t+0)$ of the following local Riemann problem

$$\begin{cases} \partial_\tau \mathbf{U} + \partial_x \mathbf{F}_1 = 0, & \tau > t, \\ \mathbf{U}(x, t) = \begin{cases} \mathbf{U}_{i,j}(t), & \text{if } x < x_{i+\frac{1}{2}}, \\ \mathbf{U}_{i+1,j}(t), & \text{if } x > x_{i+\frac{1}{2}} \end{cases} \end{cases}$$

and $\mathbf{U}_{i,j+\frac{1}{2}}^{RP}$ is the solution at $(y_{j+\frac{1}{2}}, t+0)$ of local Riemann problem

$$\begin{cases} \partial_\tau \mathbf{U} + \partial_y \mathbf{F}_2 = 0, & \tau > t, \\ \mathbf{U}(y, t) = \begin{cases} \mathbf{U}_{i,j}(t), & \text{if } y < y_{j+\frac{1}{2}}, \\ \mathbf{U}_{i,j+1}(t), & \text{if } y > y_{j+\frac{1}{2}}. \end{cases} \end{cases}$$

3. Consistency

Before proving the consistency of finite volume method (2.13) we formulate a physically reasonable assumption.

Assumption 3.1. We assume that

$$0 < \underline{\rho} \leq \rho_h, \quad E_h \leq \bar{E} \quad \text{uniformly for } h \rightarrow 0, \quad t \in [0, T], \quad (3.1)$$

where $\underline{\rho}, \bar{E}$ are positive constants.

Lemma 3.1. Under Assumption 3.1 it holds

$$0 < \underline{\rho} \leq \rho_h \leq \bar{\rho}, \quad |\mathbf{u}| \leq \bar{u}, \quad 0 < \underline{p} \leq p_h \leq \bar{p}, \quad (3.2)$$

$$|\mathbf{m}| \leq \bar{m}, \quad 0 < \underline{E} \leq E_h \leq \bar{E}, \quad 0 < \underline{\vartheta} \leq \vartheta_h \leq \bar{\vartheta} \quad (3.3)$$

uniformly for $h \rightarrow 0, t \in [0, T]$ with positive constants $\underline{\rho}, \bar{\rho}, \bar{u}, \underline{p}, \bar{p}, \bar{m}, \underline{E}, \bar{E}, \underline{\vartheta}, \bar{\vartheta}$, where $\vartheta := \frac{p}{\rho}$ is the temperature.

Proof. Here we only give the idea and framework of the proof. More details could be found in [15].

It is easy to observe that

$$p = (\gamma - 1) \left[E - \frac{|m|^2}{2\rho} \right] \leq (\gamma - 1)E \leq (\gamma - 1)\bar{E}, \quad |\mathbf{u}|^2 \leq \frac{2E}{\rho} \leq \frac{2\bar{E}}{\underline{\rho}},$$

which implies

$$\bar{p} = (\gamma - 1)\bar{E}, \quad \bar{u} = \sqrt{\frac{2\bar{E}}{\underline{\rho}}}, \quad \bar{\vartheta} = \frac{\bar{p}}{\underline{\rho}}.$$

On the other hand, we use the fact that the finite volume method (2.13) is entropy stable, cf. [25, 6]. Thus, using the renormalized entropy

$$\eta = \rho\chi(S), \quad \chi'(z) \geq 0, \quad \chi(z) = \begin{cases} < 0, & \text{if } z \leq z_0, \\ = 0, & \text{if } z \geq z_0, \end{cases}$$

$$z_0 = (\gamma - 1) \ln(1/\bar{C}), \quad \bar{C} := \max_K \frac{\rho_K(0)}{\vartheta_K(0)^{1/(\gamma-1)}}$$

implies

$$0 < \rho_h \leq \bar{C}\vartheta_h^{1/(\gamma-1)}. \quad (3.4)$$

Consequently, we obtain

$$0 < \underline{\rho}^\gamma \leq \rho_h^\gamma \leq \bar{C}^{\gamma-1} \rho_h \vartheta_h = \bar{C}^{\gamma-1} p_h \leq \bar{C}^{\gamma-1} (\gamma - 1) E_h \leq \bar{C}^{\gamma-1} (\gamma - 1) \bar{E},$$

which gives

$$\bar{\rho} = (\bar{C}^{\gamma-1} (\gamma - 1) \bar{E})^{1/\gamma}, \quad \bar{m} = \sqrt{\bar{\rho} \bar{E}}, \quad \underline{p} = \frac{\underline{\rho}^\gamma}{\bar{C}^{\gamma-1}}, \quad \underline{E} = \frac{\underline{\rho}^\gamma}{(\gamma - 1) \bar{C}^{\gamma-1}}, \quad \underline{\vartheta} = \frac{\underline{p}}{\underline{\rho}}$$

and concludes the proof. \square

Note that Assumption 3.1 is equivalent to the strict convexity of mathematical entropy function (2.3), see Appendix B.

Lemma 3.2. *Under Assumption 3.1 it holds ¹*

$$(1) \quad \|\llbracket \mathbf{F}_h \rrbracket \cdot \mathbf{n}\| \lesssim \|\llbracket \mathbf{U}_h \rrbracket\| < \infty, \quad \|\llbracket \mathbf{V}_h \rrbracket\| \lesssim \|\llbracket \mathbf{U}_h \rrbracket\| < \infty, \quad \|\llbracket \mathbf{U}_h \rrbracket\| \lesssim \|\llbracket \mathbf{V}_h \rrbracket\| < \infty.$$

$$(2) \quad \nabla_{\mathbf{U}}^2 \eta(\mathbf{U}_h) \geq \underline{\eta} I \text{ with a positive constant } \underline{\eta}.$$

Here $\mathbf{V} = (\rho, \mathbf{u}, p)^T$ and $\mathbf{F}_h = \mathbf{F}(\mathbf{U}_h)$, $\boldsymbol{\nu}_h = \boldsymbol{\nu}(\mathbf{U}_h)$, $\mathbf{V}_h = \mathbf{V}(\mathbf{U}_h)$.

Proof. Lemma 3.1 implies the boundedness of $\{\mathbf{U}_h\}$ and $\{\mathbf{V}_h\}$.

¹We use the notations $\|\cdot\|$, $\|\cdot\|_2$ and $|\cdot|$ for the L^1 -, L^2 -norm and the absolute value, respectively.

- (1) Since $\mathbf{F}(\mathbf{U}), \boldsymbol{\nu}(\mathbf{U}), \mathbf{V}(\mathbf{U})$ are smooth with respect to \mathbf{U} and $\mathbf{U}(\mathbf{V})$ is smooth with respect to \mathbf{V} , the inequalities in (1) hold.
- (2) In [24] Harten proved that $\nabla_{\mathbf{U}}^2 \eta(\mathbf{U})$ is positive definite for all \mathbf{U} . Assume that in (2) $\eta = 0$. Then there exists a subsequence \mathbf{U}_{h_n} satisfying $\nabla_{\mathbf{U}}^2 \eta(\mathbf{U}_{h_n}) \leq \frac{1}{n}$. Since $\{\mathbf{U}_{h_n}\}$ is a bounded set, there exists a subsequence $\mathbf{U}_{h_{n_k}}$ which converges to some \mathbf{U} . Hence, we get $\nabla_{\mathbf{U}}^2 \eta(\mathbf{U}) = 0$, which is a contradiction.

□

Remark 3.1. Detailed calculations to the proof of statement (1) for Lemma 3.2 are presented in Appendix A. The explicit expression of the lower bound $\underline{\eta}$ of $\nabla_{\mathbf{U}}^2 \eta(\mathbf{U}_h)$ is derived in Appendix B.

3.1. Entropy inequality

In [25] Harten proved that the Godunov finite volume method based on the exact solution of the Riemann problem satisfies the entropy inequality (in one-dimensional case)

$$\eta(\mathbf{U}_i(t_{n+1})) - \eta(\mathbf{U}_i(t_n)) \leq \frac{\tau}{\Delta x} \left(-\mathbf{q}(\mathbf{U}_{i+1/2}^{RP}) + \mathbf{q}(\mathbf{U}_{i-1/2}^{RP}) \right),$$

where $\tau = t_{n+1} - t_n$ is the time-step. Generalizing to multi-dimensions and writing it in the semi-discretization form give

$$\int_K \frac{d}{dt} \eta_K(t) \, d\mathbf{x} + \sum_{\partial K \cap \partial L \neq \emptyset} \int_{\partial K \cap \partial L} \mathbf{q}(\mathbf{U}_{\sigma_{K,L}}^{RP}) \cdot \mathbf{n}_K \, dS_{\mathbf{x}} \leq 0. \quad (3.5)$$

Further, we get the equivalent weak form

$$\int_{\Omega} \phi \frac{d}{dt} \eta_h \, d\mathbf{x} - \sum_{\sigma \in \Sigma_{\text{int}}} \int_{\sigma} \mathbf{q}(\mathbf{U}_{\sigma}^{RP}) \cdot \mathbf{n} [[\phi]] \, dS_{\mathbf{x}} \leq 0 \quad (3.6)$$

with $\phi \in \mathcal{Q}_h(\Omega)$, $\phi \geq 0$ and $\eta_h = \eta(\mathbf{U}_h)$.

On the other hand, Chen and Shu in [6] showed that the Godunov finite volume method is entropy stable, i.e.

$$\int_K \frac{d}{dt} \eta_K(t) \, d\mathbf{x} + \sum_{\partial K \cap \partial L \neq \emptyset} \int_{\partial K \cap \partial L} \mathbf{Q}_{\sigma} \cdot \mathbf{n}_K \, dS_{\mathbf{x}} \leq 0 \quad (3.7)$$

with

$$\mathbf{Q}_{\sigma} \cdot \mathbf{n}_K = \{\boldsymbol{\nu}\}_{\sigma} \cdot (\mathbf{F}(\mathbf{U}_{\sigma}^{RP}) \cdot \mathbf{n}_K) - \{\boldsymbol{\psi}\}_{\sigma} \cdot \mathbf{n}_K.$$

Writing explicitly the entropy dissipation we get

$$\int_K \frac{d}{dt} \eta_K(t) \, d\mathbf{x} + \sum_{\partial K \cap \partial L \neq \emptyset} \int_{\partial K \cap \partial L} \mathbf{Q}_\sigma \cdot \mathbf{n}_K \, dS\mathbf{x} = \frac{1}{2} \sum_{\partial K \cap \partial L \neq \emptyset} \int_{\partial K \cap \partial L} r_\sigma \, dS\mathbf{x}, \quad (3.8)$$

where

$$\begin{aligned} r_\sigma &= [[\boldsymbol{\nu}]]_\sigma \cdot (\mathbf{F}(\mathbf{U}_\sigma^{RP}) \cdot \mathbf{n}) - [[\boldsymbol{\psi}]]_\sigma \cdot \mathbf{n} \\ &= [[\boldsymbol{\nu}]]_\sigma \cdot \int_{-1/2}^{1/2} \left[\mathbf{F}(\mathbf{U}(\boldsymbol{\nu}_\sigma^{RP})) - \mathbf{F}(\mathbf{U}(\boldsymbol{\nu}(s))) \right] \cdot \mathbf{n} \, ds := [[\boldsymbol{\nu}]]_\sigma \cdot \mathbf{D}_\sigma \cdot [[\boldsymbol{\nu}]]_\sigma, \end{aligned}$$

and $\boldsymbol{\nu}(s) = \{\boldsymbol{\nu}\}_\sigma + s [[\boldsymbol{\nu}]]_\sigma$. Note that matrix \mathbf{D}_σ is symmetric because $\frac{d\mathbf{F}_i}{d\boldsymbol{\nu}}$, ($i = 1, \dots, d$) is symmetric. Hence, (3.7) implies $r_\sigma \leq 0$, i.e., $\mathbf{v} \cdot \mathbf{D}_\sigma \cdot \mathbf{v} \leq 0$ for any $\mathbf{v} \in \mathbb{R}^{d+2}$. Combining Lemma 3.1 we have $\mathbf{v} \cdot \mathbf{D}_\sigma \cdot \mathbf{v} \leq \underline{d} < 0$ uniformly for $h \rightarrow 0$. Therefore, it holds

$$\begin{aligned} & \int_K \frac{d}{dt} \eta_K(t) \, d\mathbf{x} + \sum_{\partial K \cap \partial L \neq \emptyset} \int_{\partial K \cap \partial L} \mathbf{Q}_\sigma \cdot \mathbf{n}_K \, dS\mathbf{x} \\ & \leq \frac{\underline{d}}{2} \sum_{\partial K \cap \partial L \neq \emptyset} \int_{\partial K \cap \partial L} \| [[\boldsymbol{\nu}]]_\sigma \|_2^2 \, dS\mathbf{x} \leq \frac{\underline{d}\eta}{2} \sum_{\partial K \cap \partial L \neq \emptyset} \int_{\partial K \cap \partial L} \| [[\mathbf{U}]]_\sigma \|_2^2 \, dS\mathbf{x}, \end{aligned}$$

which implies the weak BV estimate

$$\int_0^\tau \sum_{\sigma \in \Sigma_{\text{int}}} \int_\sigma \| [[\mathbf{U}]]_\sigma \|_2^2 \, dS\mathbf{x} dt \leq -\frac{1}{\underline{d}\eta} \left(\int_\Omega \eta_h(0) \, d\mathbf{x} - \int_\Omega \eta_h(\tau) \, d\mathbf{x} \right) \leq C, \quad (3.9)$$

where C is a positive constant depending on $\underline{d}, \underline{\eta}, \underline{\rho}, \bar{E}$. Realizing that $\sum_{\sigma \in \Sigma_{\text{int}}} \int_\sigma \| [[\mathbf{U}]]_\sigma \|_2^2 / h \, dS\mathbf{x}$ represents H_0^1 -seminorm, we have the following interpretation of (3.9). It tells us that

$$\|\mathbf{U}\|_{L^2(0,T;H_0^1(\Omega))} \lesssim h^{-1/2}. \quad (3.10)$$

3.2. Difference between \mathbf{U}^{RP} and $\mathbf{U}_L, \mathbf{U}_R$

For the sake of convenience, we write (u, v, w) in place of \mathbf{u} . Taking x -direction as an example, our strategy is to study the difference between $\mathbf{U}(x/t; \mathbf{U}_L, \mathbf{U}_R)$ and \mathbf{U}_K , ($K = L, R$), where $\mathbf{U}(x/t; \mathbf{U}_L, \mathbf{U}_R)$ is the solution along the line x/t of the following Riemann problem

$$\begin{cases} \partial_t \mathbf{U} + \partial_x \mathbf{F}_1 = 0, & t > 0, \\ \mathbf{U}(x, 0) = \begin{cases} \mathbf{U}_L, & \text{if } x < 0, \\ \mathbf{U}_R, & \text{if } x > 0, \end{cases} \end{cases} \quad (3.11)$$

where $\mathbf{U}_L, \mathbf{U}_R$ are constant. Once $\|\mathbf{U}(x/t; \mathbf{U}_L, \mathbf{U}_R) - \mathbf{U}_K\|$ is clearly known, then with the definition of $\mathbf{U}^{RP} = \mathbf{U}(0; \mathbf{U}_L, \mathbf{U}_R)$, we can directly estimate $\|\mathbf{U}^{RP} - \mathbf{U}_K\|$.

We divide the $x-t$ domain into four parts separated by the left and right (non-linear) waves and the middle (linear-degenerated) waves. Figure 3.1 shows the possible wave patterns including left rarefaction, right rarefaction; left shock, right shock; left rarefaction, right shock; left shock, right rarefaction. Due to Lemma 3.2, the estimate of $\|\mathbf{U}(x/t; \mathbf{U}_L, \mathbf{U}_R) - \mathbf{U}_K\|$ reduces to estimating $\|\mathbf{V}_{*M} - \mathbf{V}_K\|$ and $\|\mathbf{V}_{fan} - \mathbf{V}_K\|$ with $M = L, R$ and $K = L, R$.

Moreover, the Riemann Invariants and Rankine-Hugoniot conditions imply that $v = v_L, w = w_L$ before the middle wave and $v = v_R, w = w_R$ after the middle wave. Hence, we only need to study the change of ρ, u, p .

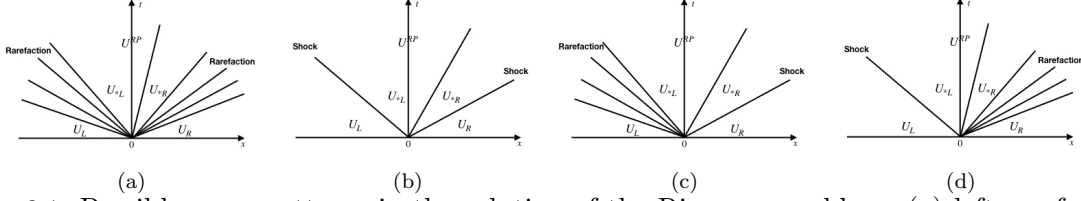


Figure 3.1: Possible wave patterns in the solution of the Riemann problem: (a) left rarefaction, right rarefaction; (b) left shock, right shock; (c) left rarefaction, right shock; (d) left shock, right rarefaction.

3.2.1. Preliminaries

Here we list some results which will be used for the estimates of $\|\mathbf{V}_{*M} - \mathbf{V}_K\|$ and $\|\mathbf{V}_{fan} - \mathbf{V}_K\|$, cf. [20, 30].

Proposition 3.1. (solution for p_* and u_*) *The solution for pressure p_* of the Riemann problem (3.11) is given by the root of the algebraic equation*

$$f(p, \mathbf{U}_L, \mathbf{U}_R) := f_L(p, \mathbf{U}_L) + f_R(p, \mathbf{U}_R) + \Delta u = 0, \quad \Delta u = u_R - u_L, \quad (3.12)$$

where the function $f_K, (K = L \text{ or } R)$ is given by

$$f_K(p, \mathbf{U}_K) = \begin{cases} f_s(p, \mathbf{U}_K), & \text{if } p > p_K \text{ shock,} \\ f_r(p, \mathbf{U}_K), & \text{if } p \leq p_K \text{ rarefaction} \end{cases}$$

with

$$f_s(p, \mathbf{U}_K) = (p - p_K) \left(\frac{A_K}{p + B_K} \right)^{1/2}, \quad A_K = \frac{2}{(\gamma + 1)\rho_K}, \quad (3.13)$$

$$f_r(p, \mathbf{U}_K) = \frac{2a_K}{(\gamma - 1)} \left[\left(\frac{p}{p_K} \right)^{\frac{\gamma-1}{2\gamma}} - 1 \right], \quad B_K = \frac{\gamma - 1}{\gamma + 1} p_K. \quad (3.14)$$

The solution for the velocity u_* in the star region is

$$u_* = \frac{1}{2}(u_L + u_R) + \frac{1}{2}[f_R(p_*) - f_L(p_*)]. \quad (3.15)$$

Remark 3.2. *More precisely, u_*, p_* satisfy*

$$u_* = u_L - f_L(p_*, \mathbf{U}_L), \quad u_* = u_R - f_R(p_*, \mathbf{U}_R). \quad (3.16)$$

*For the right shock the density ρ_{*R} is found to be*

$$\rho_{*R} = \rho_R \left[\frac{\frac{p_*}{p_R} + \frac{\gamma-1}{\gamma+1}}{\frac{\gamma-1}{\gamma+1} \frac{p_*}{p_R} + 1} \right] \quad (3.17)$$

and the shock speed is

$$s_R = u_R + a_R \left[\frac{\gamma+1}{2\gamma} \frac{p_*}{p_R} + \frac{\gamma-1}{2\gamma} \right]^{1/2}. \quad (3.18)$$

Proposition 3.2. *It holds*

$$f'_K > 0, \quad f''_K < 0, \quad K = L, R. \quad (3.19)$$

3.2.2. Estimates

We start by studying the solution inside the rarefaction fan.

Lemma 3.3. *Assume \mathbf{U}_L and \mathbf{U}_R are connected with the left rarefaction. Denote*

$$\mathbf{U}_{Lfan} := (\rho_*, \rho_* u_*, E(\rho_*, u_*, p_*))^T$$

as the value inside left rarefaction fan. Then it holds

$$\rho_L \geq \rho_* \geq \rho_R, \quad u_L \leq u_* \leq u_R, \quad p_L \geq p_* \geq p_R. \quad (3.20)$$

Proof. Since \mathbf{U}_L and \mathbf{U}_R are connected with the left rarefaction, then it holds

$$p_L \geq p_* \geq p_R, \quad u_* = u_L - f_r(p_*, \mathbf{U}_L), \quad u_R = u_L - f_r(p_R, \mathbf{U}_L),$$

where f_r is defined in (3.14). From $p_L \geq p_* \geq p_R$ and $f_r(p_L, \mathbf{U}_L) = 0$, $f'_r > 0$ we have

$$u_L \leq u_* \leq u_R.$$

On the other hand, with the Riemann Invariant $S := \ln(p/\rho^\gamma)$ we have

$$\rho_L \geq \rho_* \geq \rho_R,$$

which concludes the proof. □

Consequently, the value inside left-rarefaction-fan (\mathbf{V}_{Lfan}) can be bounded by the left and right side values ($\mathbf{V}_L, \mathbf{V}_R$). Clearly, it is also true for the right rarefaction wave. Thus, $\|\mathbf{V}_{fan} - \mathbf{V}_K\|$ can be controlled by $\|\mathbf{V}_{*M} - \mathbf{V}_K\|$. Hence, we concentrate on $\|\mathbf{V}_{*M} - \mathbf{V}_K\|$ and analyze it case by case:

- (a) left rarefaction, right rarefaction; (c) left rarefaction, right shock;
(b) left shock, right shock; (d) left shock, right rarefaction.

Lemma 3.4 (Left rarefaction, right rarefaction). *Assume the initial data $\mathbf{U}_L, \mathbf{U}_R$ generate left and right rarefaction waves. Then it holds*

$$|u_* - u_K| \leq [[u]], \quad (3.21)$$

$$0 \leq p_K - p_* \leq \rho_K a_K [[u]], \quad (3.22)$$

$$|\rho_{*K} - \rho_M| \leq \rho_K a_K^{-1} [[u]] + |[[\rho]]|, \quad (3.23)$$

where $K = L, R$ and $M = L, R$.

Proof. Since the initial data $\mathbf{U}_L, \mathbf{U}_R$ generate left and right rarefaction waves, we have

$$p_* \leq p_L, \quad p_* \leq p_R \quad (3.24)$$

and

$$u_* = u_L - f_r(p_*, \mathbf{U}_L), \quad u_* = u_R + f_r(p_*, \mathbf{U}_R). \quad (3.25)$$

Because of $f_r(p_K, \mathbf{U}_K) = 0$, ($K = L, R$) and $f_r' > 0$, it holds

$$u_* \geq u_L - f_r(p_L, \mathbf{U}_L) = u_L, \quad u_* \leq u_R + f_r(p_R, \mathbf{U}_R) = u_R, \quad (3.26)$$

which gives

$$0 \leq u_* - u_L \leq [[u]], \quad 0 \leq u_R - u_* \leq [[u]]. \quad (3.27)$$

Consider the left rarefaction wave. The Riemann Invariant

$$u_L + \frac{2a_L}{\gamma - 1} = u_* + \frac{2a_{*L}}{\gamma - 1}$$

gives

$$0 \leq a_L - a_{*L} = \frac{\gamma - 1}{2}(u_* - u_L) \leq \frac{\gamma - 1}{2} [[u]]. \quad (3.28)$$

On the other hand, with the help of the Riemann Invariant S we have

$$\begin{aligned} a_L - a_{*L} &= \gamma^{1/2} e^{S_L/(2\gamma)} \left(p_L^{(\gamma-1)/(2\gamma)} - p_*^{(\gamma-1)/(2\gamma)} \right) = \gamma^{1/2} e^{S_L/(2\gamma)} \frac{\gamma - 1}{2\gamma} p_1^{-(\gamma+1)/(2\gamma)} (p_L - p_*) \\ &\geq \gamma^{1/2} e^{S_L/(2\gamma)} \cdot \frac{\gamma - 1}{2\gamma} \cdot p_L^{-(\gamma+1)/(2\gamma)} (p_L - p_*) = \frac{\gamma^{1/(\gamma-1)}(\gamma - 1)}{2} e^{S_L/(\gamma-1)} a_L^{-(\gamma+1)/(\gamma-1)} (p_L - p_*) \end{aligned}$$

and

$$\begin{aligned} a_L - a_{*L} &= \gamma^{1/2} e^{S_L/2} \left(\rho_L^{(\gamma-1)/2} - \rho_{*L}^{(\gamma-1)/2} \right) = \gamma^{1/2} e^{S_L/2} \frac{\gamma - 1}{2} \rho_1^{(\gamma-3)/2} (\rho_L - \rho_{*L}) \\ &\geq \gamma^{1/2} e^{S_L/2} \frac{\gamma - 1}{2} \rho_L^{(\gamma-3)/2} (\rho_L - \rho_{*L}) = \frac{\gamma^{1/(\gamma-1)}(\gamma - 1)}{2} e^{S_L/(\gamma-1)} a_L^{(\gamma-3)/(\gamma-1)} (\rho_L - \rho_{*L}), \end{aligned}$$

where $p_1 \in (p_*, p_L)$, $\rho_1 \in (\rho_{*L}, \rho_L)$. Hence, we obtain

$$\begin{aligned} 0 \leq p_L - p_* &\leq \gamma^{-1/(\gamma-1)} \cdot e^{-S_L/(\gamma-1)} a_L^{(\gamma+1)/(\gamma-1)} [[u]] = \rho_L a_L [[u]], \\ 0 \leq \rho_L - \rho_{*L} &\leq \gamma^{-1/(\gamma-1)} e^{-S_L/(\gamma-1)} a_L^{(3-\gamma)/(\gamma-1)} [[u]] = \rho_L a_L^{-1} [[u]]. \end{aligned}$$

Analogously, for the right rarefaction wave we obtain

$$0 \leq p_R - p_* \leq \rho_R a_R [[u]], \quad 0 \leq \rho_R - \rho_{*R} \leq \rho_R a_R^{-1} [[u]].$$

Consequently,

$$\begin{aligned} |\rho_R - \rho_{*L}| &\leq |\rho_R - \rho_L| + |\rho_L - \rho_{*L}| \leq \rho_L a_L^{-1} [[u]] + |[[\rho]]|, \\ |\rho_L - \rho_{*R}| &\leq |\rho_R - \rho_L| + |\rho_R - \rho_{*R}| \leq \rho_R a_R^{-1} [[u]] + |[[\rho]]|, \end{aligned}$$

which concludes the proof. \square

Lemma 3.5 (Left shock, right shock). *Assume the initial data $\mathbf{U}_L, \mathbf{U}_R$ generate left and right shock waves. Then it holds*

$$|u_* - u_K| < |[[u]]|, \tag{3.29}$$

$$0 < p_* - p_K < (\gamma \rho_K |[[u]]| + \rho_K a_K) |[[u]]|, \tag{3.30}$$

$$|\rho_{*K} - \rho_M| < a_K^{-2} (\gamma \rho_K |[[u]]| + \rho_K a_K) |[[u]]| + |[[\rho]]|, \tag{3.31}$$

where $K = L, R$ and $M = L, R$.

Proof. Since the initial data $\mathbf{U}_L, \mathbf{U}_R$ generate left and right shock waves, we have

$$p_* > p_L, \quad p_* > p_R, \tag{3.32}$$

where s_L, s_R are the velocities of the left and right shocks respectively. According to

$$u_* = u_L - f_s(p_*, \mathbf{U}_L), \quad u_* = u_R + f_s(p_*, \mathbf{U}_R)$$

and $f_s(p_K, \mathbf{U}_K) = 0$, ($K = L, R$), $f'_s > 0$, we obtain

$$u_* < u_L - f_s(p_L, \mathbf{U}_L) = u_L, \quad u_* > u_R + f_s(p_*, \mathbf{U}_R) = u_R, \tag{3.33}$$

which means

$$0 < u_L - u_* < -[[u]], \quad 0 < u_* - u_R < -[[u]]. \tag{3.34}$$

Consider the right shock wave. With $u_* = u_R + f_s(p_*, \mathbf{U}_R)$ and

$$s_R = u_R + a_R \left[\frac{(\gamma+1)p_*}{2\gamma p_R} + \frac{(\gamma-1)}{2\gamma} \right]^{1/2} < u_R + a_R \left(\frac{p_*}{p_R} \right)^{1/2},$$

consequently we derive after some algebraic manipulations

$$\begin{aligned} p_* - p_R &= \left[\frac{(\gamma + 1)p_* + (\gamma - 1)p_R}{2/\rho_R} \right]^{1/2} (u_* - u_R) = \rho_R (s_R - u_R) (u_* - u_R) \\ &< \rho_R (s_R - u_R) |[u]| < \rho_R a_R |[u]| \left(\frac{p_*}{p_R} \right)^{1/2}. \end{aligned}$$

Thus,

$$\frac{p_*}{p_R} - \frac{\rho_R a_R |[u]|}{p_R} \left(\frac{p_*}{p_R} \right)^{1/2} - 1 < 0,$$

which gives

$$\left(\frac{p_*}{p_R} \right)^{1/2} < \frac{1}{2} \left[\frac{\rho_R a_R |[u]|}{p_R} + \sqrt{\left(\frac{\rho_R a_R |[u]|}{p_R} \right)^2 + 4} \right] < \frac{\rho_R a_R |[u]|}{p_R} + 2.$$

Hence, we obtain

$$p_* - p_R < (\gamma \rho_R |[u]| + \rho_R a_R) |[u]|.$$

On the other hand, using

$$\rho_{*R} = \rho_R \left[\frac{\frac{p_*}{p_R} + \frac{\gamma-1}{\gamma+1}}{\frac{\gamma-1}{\gamma+1} \frac{p_*}{p_R} + 1} \right]$$

we obtain

$$\begin{aligned} \rho_{*R} - \rho_R &= \left[\frac{2\rho_R}{(\gamma - 1)p_* + (\gamma + 1)p_R} \right] (p_* - p_R) < \left[\frac{2\rho_R}{(\gamma - 1)p_R + (\gamma + 1)p_R} \right] (p_* - p_R) \\ &= a_R^{-2} (p_* - p_R) \leq a_R^{-2} (\gamma \rho_R |[u]| + \rho_R a_R) |[u]|, \end{aligned}$$

which yields $\rho_{*R} - \rho_R > 0$.

Analogously analyzing the left shock wave we obtain

$$\begin{aligned} 0 &< p_* - p_L < (\gamma \rho_L |[u]| + \rho_L a_L) |[u]|, \\ 0 &< \rho_{*L} - \rho_L < a_L^{-2} (\gamma \rho_L |[u]| + \rho_L a_L) |[u]|. \end{aligned}$$

Further, we have

$$\begin{aligned} |\rho_{*L} - \rho_R| &< a_L^{-2} (\gamma \rho_L |[u]| + \rho_L a_L) |[u]| + |[\rho]|, \\ |\rho_{*R} - \rho_L| &< a_R^{-2} (\gamma \rho_R |[u]| + \rho_R a_R) |[u]| + |[\rho]|, \end{aligned}$$

which concludes the proof. \square

Lemma 3.6 (Left rarefaction, right shock). *Assume the initial data $\mathbf{U}_L, \mathbf{U}_R$ generate left rarefaction waves and right shock waves. Then it holds*

$$0 \leq u_* - u_K < (\rho_R a_R)^{-1} |[[p]]| + |[[u]]|, \quad (3.35)$$

$$|p_K - p_*| < |[[p]]|, \quad (3.36)$$

$$|\rho_{*K} - \rho_M| \leq (p_K/p_R)^{(\gamma-1)/\gamma} a_K^{-2} |[[p]]| + |[[\rho]]|, \quad (3.37)$$

where $K = L, R$ and $M = L, R$.

Proof. Since the initial data $\mathbf{U}_L, \mathbf{U}_R$ generate left rarefaction waves and right shock waves, we have

$$p_* \leq p_L, \quad p_* > p_R, \quad u_L - a_L \leq u_* - a_{*L}, \quad u_* + a_{*R} > S_R > u_R + a_R \quad (3.38)$$

and

$$u_* = u_L - f_r(p_*, \mathbf{U}_L), \quad u_* = u_R + f_s(p_*, \mathbf{U}_R). \quad (3.39)$$

This leads to

$$0 \leq p_L - p_* \leq -[[p]], \quad 0 < p_* - p_R \leq -[[p]] \quad (3.40)$$

and

$$u_* \geq u_L - f_r(p_L, \mathbf{U}_L) = u_L, \quad u_* > u_R + f_r(p_R, \mathbf{U}_R) = u_R. \quad (3.41)$$

Consider the right shock wave. Realizing that

$$\rho_{*R} = \rho_R \left[\frac{\frac{p_*}{p_R} + \frac{\gamma-1}{\gamma+1}}{\frac{\gamma-1}{\gamma+1} \frac{p_*}{p_R} + 1} \right],$$

we obtain

$$\begin{aligned} \rho_{*R} - \rho_R &= \left[\frac{2\rho_R}{(\gamma-1)p_* + (\gamma+1)p_R} \right] (p_* - p_R) \\ &< \left[\frac{2\rho_R}{(\gamma-1)p_R + (\gamma+1)p_R} \right] (p_* - p_R) = a_R^{-2} (p_* - p_R) \leq a_R^{-2} |[[p]]|, \end{aligned}$$

which also implies $\rho_{*R} - \rho_R > 0$. Since u_* satisfies $u_* = u_R + f_s(p_*, \mathbf{U}_R)$, we have

$$\begin{aligned} u_* - u_R &= \left[\frac{2/\rho_R}{(\gamma+1)p_* + (\gamma-1)p_R} \right]^{1/2} (p_* - p_R) < \left[\frac{2/\rho_R}{(\gamma+1)p_R + (\gamma-1)p_R} \right]^{1/2} (p_* - p_R) \\ &= (\gamma\rho_R p_R)^{-1/2} (p_* - p_R) \leq (\rho_R a_R)^{-1} |[[p]]|. \end{aligned}$$

Consider the left rarefaction wave. Clearly,

$$u_* - u_L < |u_* - u_R| + |[[u]]| < (\rho_R a_R)^{-1} |[[p]]| + |[[u]]|.$$

On the other hand, with the help of the Riemann Invariant S we have

$$\begin{aligned}\rho_L - \rho_{*L} &= \exp^{-S_L/\gamma} (p_L^{1/\gamma} - p_{*L}^{1/\gamma}) > 0, \\ \rho_L - \rho_{*L} &= \exp^{-S_L/\gamma} \cdot (1/\gamma) \cdot p_1^{(1-\gamma)/\gamma} (p_L - p_{*L}) < \exp^{-S_L/\gamma} \cdot (1/\gamma) \cdot p_R^{(1-\gamma)/\gamma} (p_L - p_{*L}) \\ &< \gamma^{-1} \exp^{-S_L/\gamma} \cdot p_R^{(1-\gamma)/\gamma} |[[p]]| = \left(\frac{\rho_L a_L^2}{\rho_R a_R^2} \right)^{(\gamma-1)/\gamma} a_L^{-2} = \left(\frac{p_L}{p_R} \right)^{(\gamma-1)/\gamma} a_L^{-2} |[[p]]|,\end{aligned}$$

where $p_1 \in (p_*, p_L) \subset (p_R, p_L)$. Further, we have

$$\begin{aligned}|\rho_{*L} - \rho_R| &< (p_L/p_R)^{(\gamma-1)/\gamma} a_L^{-2} |[[p]]| + |[[\rho]]|, \\ |\rho_{*R} - \rho_L| &< a_R^{-2} |[[p]]| + |[[\rho]]|,\end{aligned}$$

which concludes the proof. \square

Analogously to Lemma 3.6 the following result holds.

Lemma 3.7 (Left shock, right rarefaction). *Assume the initial data $\mathbf{U}_L, \mathbf{U}_R$ generate left shock waves and right rarefaction waves. Then it holds*

$$0 \leq u_* - u_K < (\rho_L a_L)^{-1} |[[p]]| + |[[u]]|, \quad (3.42)$$

$$|p_K - p_*| < |[[p]]|, \quad (3.43)$$

$$|\rho_{*K} - \rho_M| \leq (p_K/p_L)^{(\gamma-1)/\gamma} a_K^{-2} |[[p]]| + |[[\rho]]|, \quad (3.44)$$

where $K = L, R$ and $M = L, R$.

Combining Lemma 3.2 and Lemma 3.4 - 3.7 we finally obtain the following bounds for the Riemann problem solution.

Lemma 3.8. *Under Assumption 3.1 it holds*

$$\|\mathbf{U}_L - \mathbf{U}_\sigma^{RP}\| \lesssim \|[[\mathbf{U}_h]]\|, \quad \|\mathbf{U}_R - \mathbf{U}_\sigma^{RP}\| \lesssim \|[[\mathbf{U}_h]]\| \quad (3.45)$$

with $\sigma := L|R$.

Remark 3.3. *Lemma 3.8 implies $\|\mathbf{U}_\sigma^{RP}\| \lesssim \|\mathbf{U}_L\| + \|\mathbf{U}_R\| \leq C$ with $C = C(\rho, \bar{E})$.*

3.3. Consistency

The aim of this section is to prove the consistency of the finite volume method (2.13).

Theorem 3.1. (Consistency Formulation) *Let \mathbf{U}_h be the unique solution of the finite volume scheme (2.13) on the time interval $[0, T]$ with the initial data $\mathbf{U}_{0,h}$. Under the Assumption 3.1 we have the following results for all $\tau \in (0, T)$:*

- for all $\phi \in C^1([0, T] \times \bar{\Omega})$

$$\left[\int_{\Omega} \rho_h \phi \, d\mathbf{x} \right]_{t=0}^{t=\tau} = \int_0^{\tau} \int_{\Omega} \rho_h \partial_t \phi + \mathbf{m}_h \cdot \nabla_{\mathbf{x}} \phi \, d\mathbf{x} dt + \int_0^{\tau} e_{\rho,h}(t, \phi) \, dt; \quad (3.46)$$

- for all $\phi \in C^1([0, T] \times \bar{\Omega}; \mathbb{R}^d)$

$$\begin{aligned} \left[\int_{\Omega} \mathbf{m}_h \phi \, d\mathbf{x} \right]_{t=0}^{t=\tau} &= \int_0^{\tau} \int_{\Omega} \mathbf{m}_h \partial_t \phi + \frac{\mathbf{m}_h \otimes \mathbf{m}_h}{\rho_h} : \nabla_{\mathbf{x}} \phi \\ &\quad + p_h \operatorname{div}_{\mathbf{x}} \phi \, d\mathbf{x} dt + \int_0^{\tau} e_{\mathbf{m},h}(t, \phi) \, dt; \end{aligned} \quad (3.47)$$

- for all $\phi \in C^1([0, T] \times \bar{\Omega})$, $\phi \geq 0$

$$\left[\int_{\Omega} \eta_h \phi \, d\mathbf{x} \right]_{t=0}^{t=\tau} \leq \int_0^{\tau} \int_{\Omega} \eta_h \partial_t \phi + \mathbf{q}_h \cdot \nabla_{\mathbf{x}} \phi \, d\mathbf{x} dt + \int_0^{\tau} e_{\eta,h}(t, \phi) \, dt; \quad (3.48)$$

-

$$\int_{\Omega} E_h(\tau) \, d\mathbf{x} = \int_{\Omega} E_{0,h} \, d\mathbf{x}. \quad (3.49)$$

The errors $e_{j,h}$, ($j = \rho, \mathbf{m}, \eta$) are bounded by

$$\|e_{j,h}\|_{L^1(0,T)} \lesssim h^{1/2} \|\phi\|_{C^1([0,T] \times \bar{\Omega})} \left(\int_0^{\tau} \sum_{\sigma \in \Sigma_{\text{int}}} \int_{\sigma} \|[[U_h]]_{\sigma}\|_2^2 \, dS_{\mathbf{x}} dt \right)^{1/2}. \quad (3.50)$$

Proof. Energy conservation for (2.13) follows directly by integrating the discrete energy equation in time and applying the boundary conditions. We proceed by proving (3.46) - (3.48).

Step 1: We prove (3.46) and (3.47) by showing

$$\left[\int_{\Omega} \mathbf{U}_h \phi \, d\mathbf{x} \right]_{t=0}^{t=\tau} = \int_0^{\tau} \int_{\Omega} \mathbf{U}_h \partial_t \phi + \mathbf{F} : \nabla_{\mathbf{x}} \phi \, d\mathbf{x} dt + \int_0^{\tau} e_h(t, \phi) \, dt \quad (3.51)$$

for all $\phi \in C^1([0, T] \times \bar{\Omega}; \mathbb{R}^{d+2})$ with

$$\|e_h\|_{L^1(0,T)} \lesssim h^{1/2} \|\phi\|_{C^1([0,T] \times \bar{\Omega})} \left(\int_0^T \sum_{\sigma \in \Sigma_{\text{int}}} \int_{\sigma} \|[[U_h]]_{\sigma}\|^2 \, dS_{\mathbf{x}} dt \right)^{1/2}. \quad (3.52)$$

Realizing that

$$[[ab]] = \{a\} [[b]] + [[a]] \{b\}, \quad (3.53)$$

we obtain after some manipulations

$$\begin{aligned}
& \int_{\Omega} \mathbf{F}_h : \nabla_{\mathbf{x}} \phi \, d\mathbf{x} = \sum_K \int_K \mathbf{F}_h : \nabla_{\mathbf{x}} \phi \, d\mathbf{x} \\
&= \sum_K \int_{\partial K} \mathbf{F}_h \cdot \boldsymbol{\phi} \cdot \mathbf{n}_K \, d\mathbf{x} = - \sum_{\sigma \in \Sigma_{\text{int}}} \int_{\sigma} [[\mathbf{F}_h]] \cdot \boldsymbol{\phi} \cdot \mathbf{n} \, dS_{\mathbf{x}} \\
&= - \sum_{\sigma \in \Sigma_{\text{int}}} \int_{\sigma} \left([[\mathbf{F}_h]] \cdot (\boldsymbol{\phi} - \{\Pi_h[\boldsymbol{\phi}]\}) + [[\mathbf{F}_h]] \cdot \{\Pi_h[\boldsymbol{\phi}]\} \right) \cdot \mathbf{n} \, dS_{\mathbf{x}} \\
&= - \sum_{\sigma \in \Sigma_{\text{int}}} \int_{\sigma} \left([[\mathbf{F}_h]] \cdot (\boldsymbol{\phi} - \{\Pi_h[\boldsymbol{\phi}]\}) - [[\Pi_h[\boldsymbol{\phi}]]] \cdot \{\mathbf{F}_h\} + [[\mathbf{F}_h \cdot \Pi_h[\boldsymbol{\phi}]]] \right) \cdot \mathbf{n} \, dS_{\mathbf{x}} \\
&= \sum_{\sigma \in \Sigma_{\text{int}}} \int_{\sigma} \mathbf{F}(\mathbf{U}_{\sigma}^{RP}) \cdot \mathbf{n} \cdot [[\Pi_h[\boldsymbol{\phi}]]] \, dS_{\mathbf{x}} - \sum_{\sigma \in \Sigma_{\text{int}}} \int_{\sigma} [[\mathbf{F}_h]] \cdot \mathbf{n} \cdot (\boldsymbol{\phi} - \{\Pi_h[\boldsymbol{\phi}]\}) \, dS_{\mathbf{x}} \\
&\quad + \sum_{\sigma \in \Sigma_{\text{int}}} \int_{\sigma} (\{\mathbf{F}_h\} - \mathbf{F}(\mathbf{U}_{\sigma}^{RP})) \cdot \mathbf{n} \cdot [[\Pi_h[\boldsymbol{\phi}]]] \, dS_{\mathbf{x}}.
\end{aligned}$$

For the last equality, we have used the Gauss theorem and the no-flux or periodic boundary condition

$$\sum_{\sigma \in \Sigma_{\text{int}}} \int_{\sigma} [[\mathbf{F}_h \cdot \Pi_h[\boldsymbol{\phi}]]] \cdot \mathbf{n} \, dS_{\mathbf{x}} = \int_{\partial\Omega} \mathbf{F}_h \cdot \Pi_h[\boldsymbol{\phi}] \cdot \mathbf{n} \, dS_{\mathbf{x}} = 0. \quad (3.54)$$

Let us now consider the error terms

$$\begin{aligned}
e_1 &= \sum_{\sigma \in \Sigma_{\text{int}}} \int_{\sigma} [[\mathbf{F}_h]] \cdot \mathbf{n} \cdot (\boldsymbol{\phi} - \{\Pi_h[\boldsymbol{\phi}]\}) \, dS_{\mathbf{x}}, \\
e_2 &= - \sum_{\sigma \in \Sigma_{\text{int}}} \int_{\sigma} (\{\mathbf{F}_h\} - \mathbf{F}(\mathbf{U}_{\sigma}^{RP})) \cdot \mathbf{n} \cdot [[\Pi_h[\boldsymbol{\phi}]]] \, dS_{\mathbf{x}}.
\end{aligned}$$

Applying Lemma 3.2, i.e. $\| [[\mathbf{F}_h]] \cdot \mathbf{n} \| \lesssim \| [[\mathbf{U}_h]] \|$ and the fact

$$\| \boldsymbol{\phi} - \{\Pi_h[\boldsymbol{\phi}]\} \| \lesssim h \|\boldsymbol{\phi}\|_{C^1(\bar{\Omega})} \quad \text{for all } \mathbf{x} \in \sigma \in \Sigma_{\text{int}},$$

we have the following estimate

$$\begin{aligned}
|e_1| &\lesssim h \|\boldsymbol{\phi}\|_{C^1(\bar{\Omega})} \sum_{\sigma \in \Sigma_{\text{int}}} \int_{\sigma} \| [[\mathbf{F}_h]] \cdot \mathbf{n} \| \, dS_{\mathbf{x}} \lesssim h \|\boldsymbol{\phi}\|_{C^1(\bar{\Omega})} \sum_{\sigma \in \Sigma_{\text{int}}} \int_{\sigma} \| [[\mathbf{U}_h]] \| \, dS_{\mathbf{x}} \\
&\lesssim h \|\boldsymbol{\phi}\|_{C^1(\bar{\Omega})} \left(\sum_{\sigma \in \Sigma_{\text{int}}} \int_{\sigma} \| [[\mathbf{U}_h]] \|^2 \, dS_{\mathbf{x}} \right)^{1/2} \left(\sum_{\sigma \in \Sigma_{\text{int}}} \int_{\sigma} 1 \, dS_{\mathbf{x}} \right)^{1/2} \\
&\lesssim h^{1/2} \|\boldsymbol{\phi}\|_{C^1(\bar{\Omega})} \left(\sum_{\sigma \in \Sigma_{\text{int}}} \int_{\sigma} \| [[\mathbf{U}_h]] \|^2 \, dS_{\mathbf{x}} \right)^{1/2}.
\end{aligned}$$

Realizing that

$$\| [[\Pi_h[\phi]]] \| \lesssim h \|\phi\|_{C^1(\bar{\Omega})},$$

we derive

$$\begin{aligned} |e_2| &\leq h \|\phi\|_{C^1(\bar{\Omega})} \sum_{\sigma \in \Sigma_{\text{int}}} \int_{\sigma} \|(\{\mathbf{F}_h\} - \mathbf{F}(\mathbf{U}_{\sigma}^{RP})) \cdot \mathbf{n}\| \, dS_{\mathbf{x}} \\ &\lesssim h \|\phi\|_{C^1(\bar{\Omega})} \sum_{\sigma: =L|R \in \Sigma_{\text{int}}} \int_{\sigma} \|(\mathbf{F}(\mathbf{U}_L) - \mathbf{F}(\mathbf{U}_{\sigma}^{RP})) \cdot \mathbf{n}\| + \|(\mathbf{F}(\mathbf{U}_R) - \mathbf{F}(\mathbf{U}_{\sigma}^{RP})) \cdot \mathbf{n}\| \, dS_{\mathbf{x}} \\ &\lesssim h \|\phi\|_{C^1(\bar{\Omega})} \sum_{\sigma: =L|R \in \Sigma_{\text{int}}} \int_{\sigma} \|\mathbf{U}_L - \mathbf{U}_{\sigma}^{RP}\| + \|\mathbf{U}_R - \mathbf{U}_{\sigma}^{RP}\| \, dS_{\mathbf{x}} \\ &\lesssim h \|\phi\|_{C^1(\bar{\Omega})} \sum_{\sigma \in \Sigma_{\text{int}}} \int_{\sigma} \|[[\mathbf{U}_h]]\| \, dS_{\mathbf{x}} \lesssim h^{1/2} \|\phi\|_{C^1(\bar{\Omega})} \sum_{\sigma \in \Sigma_{\text{int}}} \int_{\sigma} \|[[\mathbf{U}_h]]\|^2 \, dS_{\mathbf{x}}. \end{aligned}$$

Hence, we can obtain

$$\begin{aligned} \left[\int_{\Omega} \mathbf{U}_h \cdot \phi \, d\mathbf{x} \right]_{t=0}^{t=\tau} &= \int_0^{\tau} \int_{\Omega} \frac{d}{dt} (\mathbf{U}_h \cdot \phi) \, d\mathbf{x} = \int_0^{\tau} \int_{\Omega} \mathbf{U}_h \cdot \partial_t \phi + \phi \cdot \frac{d}{dt} \mathbf{U}_h \, d\mathbf{x} dt \\ &= \int_0^{\tau} \int_{\Omega} \mathbf{U}_h \cdot \partial_t \phi \, d\mathbf{x} dt + \int_0^{\tau} \sum_{\sigma \in \Sigma_{\text{int}}} \int_{\sigma} \mathbf{F}(\mathbf{U}_{\sigma}^{RP}) \cdot \mathbf{n} [[\phi]] \, dS_{\mathbf{x}} \\ &= \int_0^{\tau} \int_{\Omega} \mathbf{U}_h \cdot \partial_t \phi + \mathbf{F}_h : \nabla_{\mathbf{x}} \phi \, d\mathbf{x} dt + \int_0^{\tau} e_h(t, \phi) \, dt, \end{aligned}$$

where $e_h = e_1 + e_2$ satisfies (3.52) with the help of $\|\mathbf{U}\|^2 \lesssim \|\mathbf{U}\|_2^2$.

Step 2: Indeed, using the same techniques as Step 1 to analyze (3.6) we obtain (3.48), which concludes the proof. \square

4. Convergence

In order to keep the paper self-contained we present the definition of a dissipative measure-valued solution for the Euler system (2.1), (2.6), cf. [18].

Definition 4.1. Let $\Omega \subset \mathbb{R}^d$ be a bounded domain. A parametrized probability measure $\{\mathcal{V}_{t,\mathbf{x}}\}_{(t,\mathbf{x}) \in (0,T) \times \Omega}$,

$$\mathcal{V}_{t,\mathbf{x}} \in L^{\infty}((0, T) \times \Omega, \mathcal{P}(\mathbb{R}^{d+2})), \quad \mathbb{R}^{d+2} = \{(\tilde{\rho}, \tilde{\mathbf{m}}, \tilde{\eta}) : \tilde{\rho} \in \mathbb{R}, \tilde{\mathbf{m}} \in \mathbb{R}^d, \tilde{\eta} \in \mathbb{R}\}$$

is called a dissipative measure-valued (DMV) solution of the Euler system (2.1), (2.6) with the space-periodic or no-flux boundary condition and initial condition $(\rho_0, \mathbf{m}_0, \eta_0)$ if the following holds:

- (lower bound on density and entropy)

$$\mathcal{V}_{t,\mathbf{x}} [\{\tilde{\rho} \geq 0, \tilde{\eta} \geq \underline{S}\tilde{\rho}\}] = 1 \quad \text{for a.a. } (t, \mathbf{x}) \in (0, T) \times \Omega; \quad (4.1)$$

- (energy inequality) the integral inequality

$$\int_{\Omega} \langle \mathcal{V}_{\tau, \mathbf{x}}; E(\tilde{\rho}, \tilde{\mathbf{m}}, \tilde{\eta}) \rangle d\mathbf{x} + \int_{\Omega} d\mathfrak{E}_{cd}(\tau) \leq \int_{\Omega} E(\rho_0, \mathbf{m}_0, \eta_0) d\mathbf{x} \quad (4.2)$$

holds for a.a. $0 \leq \tau \leq T$ with the energy concentration defect

$$\mathfrak{E}_{cd} \in L^{\infty}(0, T; \mathcal{M}^+(\bar{\Omega}));^2$$

- (equation of continuity)

$$\langle \mathcal{V}_{t, \mathbf{x}}; \tilde{\rho} \rangle \in C_{weak}([0, T]; L^{\gamma}(\Omega)), \quad \langle \mathcal{V}_{0, \mathbf{x}}; \tilde{\rho} \rangle = \rho_0 \quad \text{for a.a. } \mathbf{x} \in \Omega$$

and the integral equality

$$\left[\int_{\Omega} \langle \mathcal{V}_{t, \mathbf{x}}; \tilde{\rho} \rangle \phi d\mathbf{x} \right]_{t=0}^{t=\tau} = \int_0^{\tau} \int_{\Omega} \langle \mathcal{V}_{t, \mathbf{x}}; \tilde{\rho} \rangle \partial_t \phi + \langle \mathcal{V}_{t, \mathbf{x}}; \tilde{\mathbf{m}} \rangle \cdot \nabla_{\mathbf{x}} \phi d\mathbf{x} dt \quad (4.3)$$

for any $0 \leq \tau \leq T$ and any $\phi \in W^{1, \infty}((0, T) \times \Omega)$;

- (momentum equation)

$$\langle \mathcal{V}_{t, \mathbf{x}}; \tilde{\mathbf{m}} \rangle \in C_{weak}([0, T]; L^{\frac{2\gamma}{\gamma+1}}(\Omega; \mathbb{R}^d)), \quad \langle \mathcal{V}_{0, \mathbf{x}}; \tilde{\mathbf{m}} \rangle = m_0 \quad \text{for a.a. } \mathbf{x} \in \Omega$$

and the integral equality

$$\begin{aligned} \left[\int_{\Omega} \langle \mathcal{V}_{t, \mathbf{x}}; \tilde{\mathbf{m}} \rangle \phi d\mathbf{x} \right]_{t=0}^{t=\tau} &= \int_0^{\tau} \int_{\Omega} \langle \mathcal{V}_{t, \mathbf{x}}; \tilde{\mathbf{m}} \rangle \partial_t \phi + \langle \mathcal{V}_{t, \mathbf{x}}; \frac{\tilde{\mathbf{m}} \otimes \tilde{\mathbf{m}}}{\tilde{\rho}} \rangle : \nabla_{\mathbf{x}} \phi d\mathbf{x} dt \\ &+ \int_0^{\tau} \int_{\Omega} \langle \mathcal{V}_{t, \mathbf{x}}; p(\tilde{\rho}, \tilde{\eta}) \rangle \operatorname{div}_{\mathbf{x}} \phi d\mathbf{x} dt + \int_0^{\tau} \int_{\bar{\Omega}} \nabla_{\mathbf{x}} \phi : d\mathfrak{R}_{cd}(t) dt \end{aligned} \quad (4.4)$$

for any $0 \leq \tau \leq T$ and any $\phi \in C^1([0, T] \times \bar{\Omega}; \mathbb{R}^d)$, (ϕ also satisfies $\phi \cdot \mathbf{n}|_{\partial\Omega} = 0$ when no-flux boundary condition is used), where the Reynolds concentration defect

$$\mathfrak{R}_{cd} \in L^{\infty}(0, T; \mathcal{M}^+(\bar{\Omega}; \mathbb{R}_{sym}^{d \times d}))$$

satisfies

$$\underline{d}\mathfrak{E}_{cd} \leq \operatorname{tr}[\mathfrak{R}_{cd}] \leq \bar{d}\mathfrak{E}_{cd} \quad \text{for some constants } 0 < \underline{d} \leq \bar{d}; \quad (4.5)$$

² $\mathcal{M}^+(\bar{\Omega})$ denotes the set of positive Radon measures on $\bar{\Omega}$.

- (entropy balance)

$$\begin{aligned} \int_{\Omega} \langle \mathcal{V}_{\tau_{\pm}, \mathbf{x}}; \tilde{\eta} \rangle \phi \, d\mathbf{x} &\equiv \lim_{t \rightarrow \tau_{\pm}} \int_{\Omega} \langle \mathcal{V}_{t, \mathbf{x}}; \tilde{\eta} \rangle \phi \, d\mathbf{x} \quad \text{exists for any } 0 \leq \tau < T, \\ \int_{\Omega} \langle \mathcal{V}_{0+, \mathbf{x}}; \tilde{\eta} \rangle \phi \, d\mathbf{x} &\equiv \int_{\Omega} S_0 \phi \, d\mathbf{x} \quad \text{for any } \phi \in C(\overline{\Omega}), \end{aligned}$$

and the integral inequality

$$\left[\int_{\Omega} \langle \mathcal{V}_{t, \mathbf{x}}; \tilde{\eta} \rangle \phi \, d\mathbf{x} \right]_{t=\tau_1-}^{t=\tau_2+} \leq \int_{\tau_1}^{\tau_2} \int_{\Omega} \langle \mathcal{V}_{t, \mathbf{x}}; \tilde{\eta} \rangle \partial_t \phi + \langle \mathcal{V}_{t, \mathbf{x}}; \frac{\tilde{\mathbf{m}}}{\tilde{\rho}} \tilde{\eta} \rangle \cdot \nabla_{\mathbf{x}} \phi \, d\mathbf{x} dt \quad (4.6)$$

for any $0 \leq \tau \leq T$ and any $\phi \in W^{1, \infty}((0, T) \times \Omega)$, $\phi \geq 0$.

Remark 4.1. Consider a family $\{\rho_h, \mathbf{m}_h, E_h\}_{h \downarrow 0}$ of numerical solutions generated by our finite volume method (2.13). We note that a sequence $\{\rho_h, \mathbf{m}_h, E_h\}_{h \downarrow 0}$ can be mapped uniquely to a sequence $\{\rho_h, \mathbf{m}_h, \eta_h\}_{h \downarrow 0}$. Due to Theorem 3.1 $\{\rho_h, \mathbf{m}_h, \eta_h\}_{h \downarrow 0}$ is a consistent approximation of complete Euler system. Consequently, up to a subsequence $\{\rho_{h_n}, \mathbf{m}_{h_n}, \eta_{h_n}\}_{h_n \downarrow 0}$ generates the Young measure $\{\mathcal{V}_{t, \mathbf{x}}\}_{(t, \mathbf{x}) \in (0, T) \times \Omega}$, which is a dissipative measure-valued solution of the Euler system in the sense of Definition 4.1. Following [18] the concentration defects are

$$\begin{aligned} \mathfrak{E}_{cd} &= \overline{E(\rho, \mathbf{m}, \eta)} - \langle \mathcal{V}_{\tau, \mathbf{x}}; E(\tilde{\rho}, \tilde{\mathbf{m}}, \tilde{\eta}) \rangle, \\ \mathfrak{R}_{cd} &= \frac{\overline{\mathbf{m} \otimes \mathbf{m}}}{\rho} + p(\rho, \eta) \mathbb{I} - \left\langle \mathcal{V}_{t, \mathbf{x}}; \frac{\tilde{\mathbf{m}} \otimes \tilde{\mathbf{m}}}{\tilde{\rho}} + p(\tilde{\rho}, \tilde{\eta}) \mathbb{I} \right\rangle \end{aligned}$$

with

$$\begin{aligned} E(\rho_{h_n}, \mathbf{m}_{h_n}, \eta_{h_n}) &\longrightarrow \overline{E(\rho, \mathbf{m}, \eta)} \quad \text{weakly-} (*) \text{ in } \mathcal{M}(\overline{\Omega}), \\ \frac{\mathbf{m}_{h_n} \otimes \mathbf{m}_{h_n}}{\rho_{h_n}} + p(\rho_{h_n}, \eta_{h_n}) \mathbb{I} &\longrightarrow \frac{\overline{\mathbf{m} \otimes \mathbf{m}}}{\rho} + p(\rho, \eta) \mathbb{I} \quad \text{weakly-} (*) \text{ in } \mathcal{M}(\overline{\Omega}; \mathbb{R}^{d \times d}). \end{aligned}$$

Theorem 4.1. (Weak convergence)

Let $\{\rho_h, \mathbf{m}_h, \eta_h\}_{h \downarrow 0}$ be the family of numerical solutions obtained by the finite volume method (2.13). Let Assumption 3.1 hold, i.e. $0 < \underline{\rho} \leq \rho_h, E_h \leq \overline{E}$ for some $\underline{\rho}, \overline{E}$. Then there exists a subsequence $\{\rho_{h_n}, \mathbf{m}_{h_n}, \eta_{h_n}\}_{h_n > 0}$, such that

$$(\rho_{h_n}, \mathbf{m}_{h_n}, \eta_{h_n}) \longrightarrow \langle \mathcal{V}_{t, \mathbf{x}}; (\tilde{\rho}, \tilde{\mathbf{m}}, \tilde{\eta}) \rangle \quad \text{weakly-} (*) \text{ in } L^{\infty}((0, T) \times \Omega; \mathbb{R}^{d+2}),$$

where $\{\mathcal{V}_{t, \mathbf{x}}\}_{(t, \mathbf{x}) \in (0, T) \times \Omega}$ is a DMV solution of the complete Euler system (2.1), (2.6) with

$$\mathfrak{E}_{cd} \equiv 0, \quad \mathfrak{R}_{cd} \equiv 0. \quad (4.7)$$

Proof. Under Assumption 3.1 Lemma 3.1 gives

$$\begin{aligned} \rho_h &\in L^{\infty}((0, T) \times \Omega), \quad \mathbf{m}_h \in L^{\infty}((0, T) \times \Omega), \quad \eta_h \in L^{\infty}((0, T) \times \Omega), \quad E_h \in L^{\infty}((0, T) \times \Omega), \\ \frac{\mathbf{m}_h \otimes \mathbf{m}_h}{\rho_h} &\in L^{\infty}((0, T) \times \Omega), \quad p_h \in L^{\infty}((0, T) \times \Omega), \quad \mathbf{q}_h \in L^{\infty}((0, T) \times \Omega). \end{aligned}$$

Applying the Fundamental Theorem on Young Measure [1] implies the existence of a convergent subsequence and a parameterized probability measure $\{\mathcal{V}_{t,\mathbf{x}}\}_{(t,\mathbf{x}) \in (0,T) \times \Omega}$ satisfying that $(\rho_{h_n}, \mathbf{m}_{h_n}, \eta_{h_n})$ weakly-(*) converges to $(\langle \mathcal{V}_{t,\mathbf{x}}; \tilde{\rho} \rangle, \langle \mathcal{V}_{t,\mathbf{x}}; \tilde{\mathbf{m}} \rangle, \langle \mathcal{V}_{t,\mathbf{x}}; \tilde{\eta} \rangle)$ in $L^\infty((0, T) \times \Omega)$. Moreover,

$$\frac{\mathbf{m}_{h_n} \otimes \mathbf{m}_{h_n}}{\rho_{h_n}}, \quad p_{h_n} := p(\rho_{h_n}, \eta_{h_n}), \quad E_{h_n} := E(\rho_{h_n}, \mathbf{m}_{h_n}, \eta_{h_n}), \quad \mathbf{q}_{h_n} := \mathbf{q}(\rho_{h_n}, \mathbf{m}_{h_n}, \eta_{h_n})$$

weakly-(*) converge to

$$\langle \mathcal{V}_{t,\mathbf{x}}; \frac{\tilde{\mathbf{m}} \otimes \tilde{\mathbf{m}}}{\tilde{\rho}} \rangle, \quad \langle \mathcal{V}_{t,\mathbf{x}}; p(\tilde{\rho}, \tilde{\eta}) \rangle, \quad \langle \mathcal{V}_{t,\mathbf{x}}; E(\tilde{\rho}, \tilde{\mathbf{m}}, \tilde{\eta}) \rangle, \quad \langle \mathcal{V}_{t,\mathbf{x}}; \mathbf{q}(\tilde{\rho}, \tilde{\mathbf{m}}, \tilde{\eta}) \rangle$$

in $L^\infty((0, T) \times \Omega)$, respectively. Consequently, the concentration defects vanish, i.e. $\mathfrak{E}_{cd} \equiv 0$, $\mathfrak{R}_{cd} \equiv 0$.

Hence, passing to the limit $h \rightarrow 0$, (3.46) in Theorem 3.1 gives

$$\left[\int_{\Omega} \langle \mathcal{V}_{t,\mathbf{x}}; \tilde{\rho} \rangle \phi \, d\mathbf{x} \right]_{t=0}^{t=\tau} = \int_0^\tau \int_{\Omega} \langle \mathcal{V}_{t,\mathbf{x}}; \tilde{\rho} \rangle \partial_t \phi + \langle \mathcal{V}_{t,\mathbf{x}}; \tilde{\mathbf{m}} \rangle \cdot \nabla_{\mathbf{x}} \phi \, d\mathbf{x} dt \quad (4.8)$$

for $\phi \in W^{1,\infty}((0, T) \times \Omega)$. Analogously, (3.47) and (3.48) in Theorem 3.1 yield

$$\begin{aligned} \left[\int_{\Omega} \langle \mathcal{V}_{t,\mathbf{x}}; \tilde{\mathbf{m}} \rangle \phi \, d\mathbf{x} \right]_{t=0}^{t=\tau} &= \int_0^\tau \int_{\Omega} \langle \mathcal{V}_{t,\mathbf{x}}; \tilde{\mathbf{m}} \rangle \partial_t \phi + \langle \mathcal{V}_{t,\mathbf{x}}; \frac{\tilde{\mathbf{m}} \otimes \tilde{\mathbf{m}}}{\tilde{\rho}} \rangle : \nabla_{\mathbf{x}} \phi \, d\mathbf{x} dt \\ &\quad + \int_0^\tau \int_{\Omega} \langle \mathcal{V}_{t,\mathbf{x}}; p(\tilde{\rho}, \tilde{\eta}) \rangle \operatorname{div}_{\mathbf{x}} \phi \, d\mathbf{x} dt \end{aligned}$$

for $\phi \in C^1([0, T] \times \bar{\Omega}; \mathbb{R}^d)$ and $\phi \cdot \mathbf{n} = 0$ for no-flux boundary condition, and

$$\left[\int_{\Omega} \langle \mathcal{V}_{t,\mathbf{x}}; \tilde{\eta} \rangle \phi \, d\mathbf{x} \right]_{t=\tau_1-}^{t=\tau_2+} \leq \int_{\tau_1}^{\tau_2} \int_{\Omega} \langle \mathcal{V}_{t,\mathbf{x}}; \tilde{\eta} \rangle \partial_t \phi + \langle \mathcal{V}_{t,\mathbf{x}}; \mathbf{q}(\tilde{\rho}, \tilde{\mathbf{m}}, \tilde{\eta}) \rangle \cdot \nabla_{\mathbf{x}} \phi \, d\mathbf{x} dt \quad (4.9)$$

for $\phi \in W^{1,\infty}((0, T) \times \Omega)$, respectively. Finally, (3.49) in Theorem 3.1 implies

$$\int_{\Omega} \langle \mathcal{V}_{\tau,\mathbf{x}}; E(\tilde{\rho}, \tilde{\mathbf{m}}, \tilde{\eta}) \rangle \, d\mathbf{x} = \int_{\Omega} E(\rho_0, \mathbf{m}_0, \eta_0) \, d\mathbf{x} \quad (4.10)$$

and concludes that $\{\mathcal{V}_{t,\mathbf{x}}\}_{(t,\mathbf{x}) \in (0,T) \times \Omega}$ is a DMV solution of the complete Euler system. \square

Having shown weak convergence to a DMV solution allows us to look for strong convergence to the observable quantities, such as the expected value and first variance. To this end we apply a novel technique of \mathcal{K} -convergence as introduced in [16, 18].

Theorem 4.2. (\mathcal{K} -convergence)

Let $\{\rho_h, \mathbf{m}_h, \eta_h\}_{h \downarrow 0}$ be the family of numerical solutions obtained by the finite volume method (2.13). Assumption 3.1 holds. Then there exist a subsequence $\{\rho_{h_n}, \mathbf{m}_{h_n}, \eta_{h_n}\}_{h_n \downarrow 0}$ such that

- **strong convergences of Cesàro average**

$$\frac{1}{N} \sum_{n=1}^N (\rho_{h_n}, \mathbf{m}_{h_n}, \eta_{h_n}) \longrightarrow \langle \mathcal{V}_{t,\mathbf{x}}; (\tilde{\rho}, \tilde{\mathbf{m}}, \tilde{\eta}) \rangle \quad \text{in } L^q((0, T) \times \Omega; \mathbb{R}^{d+2})$$

for $N \rightarrow \infty$ and any $1 \leq q < \infty$;

- **L^q convergence to Young measure**

$$d_{W^s} \left[\frac{1}{N} \sum_{n=1}^N \delta_{(\rho_{h_n}, \mathbf{m}_{h_n}, \eta_{h_n})}; \mathcal{V}_{t,\mathbf{x}} \right] \longrightarrow 0 \quad \text{in } L^q((0, T) \times \Omega)$$

for $N \rightarrow \infty$ and any $1 \leq q < s < \infty$;

- **L^1 convergence of the first variance**

$$\frac{1}{N} \sum_{n=1}^N \left\| (\rho_{h_n}, \mathbf{m}_{h_n}, \eta_{h_n}) - \frac{1}{N} \sum_{n=1}^N (\rho_{h_n}, \mathbf{m}_{h_n}, \eta_{h_n}) \right\| \longrightarrow 0 \quad \text{in } L^1((0, T) \times \Omega)$$

for $N \rightarrow \infty$.

Applying techniques developed in [18] we directly obtain the following strong convergence results.

Theorem 4.3. (Strong convergence)

Let $\{\rho_h, \mathbf{m}_h, \eta_h\}_{h \downarrow 0}$ be the family of numerical solutions obtained by the finite volume method (2.13) and with initial data $\rho_{0,h} = \Pi_h[\rho_0]$, $\mathbf{m}_{0,h} = \Pi_h[\mathbf{m}_0]$, $\eta_{0,h} = \Pi_h[\eta_0]$. Let Assumption 3.1 hold. Let the subsequence

$$(\rho_{h_n}, \mathbf{m}_{h_n}, \eta_{h_n}) \longrightarrow (\rho, \mathbf{m}, \eta) \quad \text{as } h \longrightarrow 0$$

in the sense specified in Theorem 4.1, where the barycenters $\rho := \langle \mathcal{V}_{t,\mathbf{x}}; \tilde{\rho} \rangle$, $\mathbf{m} := \langle \mathcal{V}_{t,\mathbf{x}}; \tilde{\mathbf{m}} \rangle$ and $\eta := \langle \mathcal{V}_{t,\mathbf{x}}; \tilde{\eta} \rangle$. Then the following holds:

- **weak solution**

If (ρ, \mathbf{m}, η) is a weak entropy solution of the Euler system with initial data $(\rho_0, \mathbf{m}_0, \eta_0)$, then

$$\mathcal{V}_{t,\mathbf{x}} = \delta_{(\rho(t,\mathbf{x}), \mathbf{m}(t,\mathbf{x}), \eta(t,\mathbf{x}))} \quad \text{for a.a. } (t, \mathbf{x}) \in (0, T) \times \Omega$$

and the strong convergence holds, i.e.

$$\begin{aligned} (\rho_{h_n}, \mathbf{m}_{h_n}, \eta_{h_n}) &\longrightarrow (\rho, \mathbf{m}, \eta) && \text{in } L^q((0, T) \times \Omega; \mathbb{R}^{d+2}) \\ E(\rho_{h_n}, \mathbf{m}_{h_n}, \eta_{h_n}) &\longrightarrow E(\rho, \mathbf{m}, \eta) && \text{in } L^q((0, T) \times \Omega) \end{aligned}$$

for any $1 \leq q < \infty$.

- **classical solution**

Let $\Omega \subset \mathbb{R}^d$ be a bounded Lipschitz domain and (ρ, \mathbf{m}, η) such that

$$\rho, \eta \in C^1([0, T] \times \bar{\Omega}), \quad \mathbf{m} \in C^1([0, T] \times \bar{\Omega}; \mathbb{R}^d), \quad \rho \geq \underline{\rho} > 0 \text{ in } [0, T] \times \bar{\Omega}.$$

Then (ρ, \mathbf{m}, η) is a classical solution to the Euler system and

$$(\rho_{h_n}, \mathbf{m}_{h_n}, \eta_{h_n}) \longrightarrow (\rho, \mathbf{m}, \eta) \quad \text{in } L^q((0, T) \times \Omega; \mathbb{R}^{d+2})$$

for any $1 \leq q < \infty$.

- **strong solution**

Let periodic boundary conditions are applied. Suppose that the Euler system admits a strong solution (ρ, \mathbf{m}, η) in the class

$$\rho, \eta \in W^{1,\infty}((0, T) \times \Omega), \quad \mathbf{m} \in W^{1,\infty}((0, T) \times \Omega; \mathbb{R}^d), \quad \rho \geq \underline{\rho} > 0 \text{ in } [0, T] \times \Omega$$

emanating from initial data $(\rho_0, \mathbf{m}_0, \eta_0)$. Then it holds

$$\begin{aligned} (\rho_{h_n}, \mathbf{m}_{h_n}, \eta_{h_n}) &\longrightarrow (\rho, \mathbf{m}, \eta) && \text{in } L^q((0, T) \times \Omega; \mathbb{R}^{d+2}) \\ E(\rho_{h_n}, \mathbf{m}_{h_n}, \eta_{h_n}) &\longrightarrow E(\rho, \mathbf{m}, \eta) && \text{in } L^q((0, T) \times \Omega) \end{aligned}$$

for any $1 \leq q < \infty$.

5. Numerical results

In this section we simulate a spiral problem, i.e. two-dimensional Riemann problem, Kelvin-Helmholtz problem and Richtmyer-Meshkov problem [22, 21] to illustrate the weak, strong and \mathcal{K} -convergence of the finite volume method (2.13).

In our computations the computational domain is $[0, 1] \times [0, 1]$ and divided into $n \times n$ uniform cells. Denote the Cesàro average of the numerical solutions and their first variance

$$\tilde{U}_{h_n} = \frac{1}{n} \sum_{j=1}^n U_{h_j}, \quad \tilde{U}_{h_n}^\dagger = \frac{1}{n} \sum_{j=1}^n |U_{h_j} - \tilde{U}_{h_n}|,$$

respectively. Let U_{h_N} be the reference solution computed on the finest mesh with $N \times N$ cells. Analogously to [19] we compute four errors

$$E_1 = \|U_{h_n} - U_{h_N}\|, \quad E_2 = \|\tilde{U}_{h_n} - \tilde{U}_{h_N}\|, \quad E_3 = \|U_{h_n}^\dagger - U_{h_N}^\dagger\|, \quad E_4 = \|W_1(\bar{\mathcal{V}}_{t,x}^n, \bar{\mathcal{V}}_{t,x}^N)\|, \quad (5.1)$$

where $\bar{\mathcal{V}}_{t,x}^n$ is the Cesàro average of the Dirac measures concentrated on numerical solution U_{h_n} . In addition, we apply the outflow boundary condition to the spiral problem and periodic boundary condition to the other two problems. Moreover, the CFL number is set to 0.9 and the adiabatic index γ is taken as 1.4.

Example 5.1 (Spiral problem). We consider one of the classical 2D Riemann problem with the initial data

$$(\rho, \mathbf{u}, p)(x, 0) = \begin{cases} (0.5, 0.5, -0.5, 5), & \text{if } x > 0.5, y > 0.5; \\ (1, 0.5, 0.5, 5), & \text{if } x < 0.5, y > 0.5; \\ (1.5, -0.5, -0.5, 5), & \text{if } x > 0.5, y < 0.5; \\ (2, -0.5, 0.5, 5), & \text{if } x < 0.5, y < 0.5. \end{cases}$$

This problem describes the interaction of four contact discontinuities (vortex sheets) with the negative sign. As time increases the four initial vortex sheets interact each other to form a spiral with the low density around the center of the domain. This is a typical cavitation phenomenon well-known in gas dynamics. We compute the solution up to the finite time $T = 2$.

Figure 5.1 shows the errors E_1, E_2, E_3, E_4 of ρ, m_1, m_2, E, S obtained on different meshes and the reference solution on a mesh with 2048×2048 cells. The errors of ρ, S are specifically listed in Tables 5.1, 5.2, respectively. Moreover, Figures 5.2, 5.3 show the contour of ρ and S obtained on different meshes, respectively.

The numerical results show that four errors are all decreasing with the refinement of mesh. This together with the pictures of the first variance indicate that $\mathcal{V}_{t,x} = \delta_{(\rho, \mathbf{m}, S)(x,t)}$ and the numerical solutions converge to the weak solution. This is in accordance with our theoretical results. We point out that the convergence rate is 1.

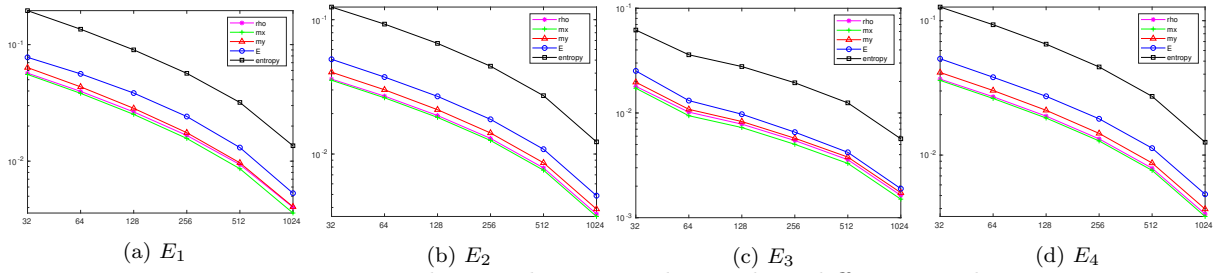


Figure 5.1: Example 5.1: the errors obtained on different meshes.

Table 5.1: Example 5.1: the errors and convergence rates for density.

n	E_1		E_2		E_3		E_4	
	error	order	error	order	error	order	error	order
32	0.0569	-	0.0361	-	0.0179	-	0.0367	-
64	0.0397	0.5189	0.0270	0.4206	0.0102	0.8165	0.0272	0.4354
128	0.0265	0.5854	0.0193	0.4795	0.0078	0.3810	0.0195	0.4790
256	0.0166	0.6698	0.0131	0.5655	0.0055	0.5199	0.0132	0.5626
512	0.0093	0.8316	0.0079	0.7299	0.0036	0.6089	0.0080	0.7258
1024	0.0040	1.2172	0.0036	1.1388	0.0016	1.1319	0.0036	1.1311

Table 5.2: Example 5.1: the errors and convergence rates for entropy.

n	E_1		E_2		E_3		E_4	
	error	order	error	order	error	order	error	order
32	0.1956	-	0.1242	-	0.0619	-	0.1263	-
64	0.1355	0.5297	0.0927	0.4216	0.0360	0.7841	0.0933	0.4372
128	0.0901	0.5882	0.0666	0.4771	0.0278	0.3734	0.0669	0.4800
256	0.0567	0.6692	0.0451	0.5634	0.0194	0.5150	0.0453	0.5632
512	0.0319	0.8297	0.0272	0.7294	0.0125	0.6370	0.0274	0.7267
1024	0.0136	1.2341	0.0123	1.1417	0.0057	1.1396	0.0125	1.1346

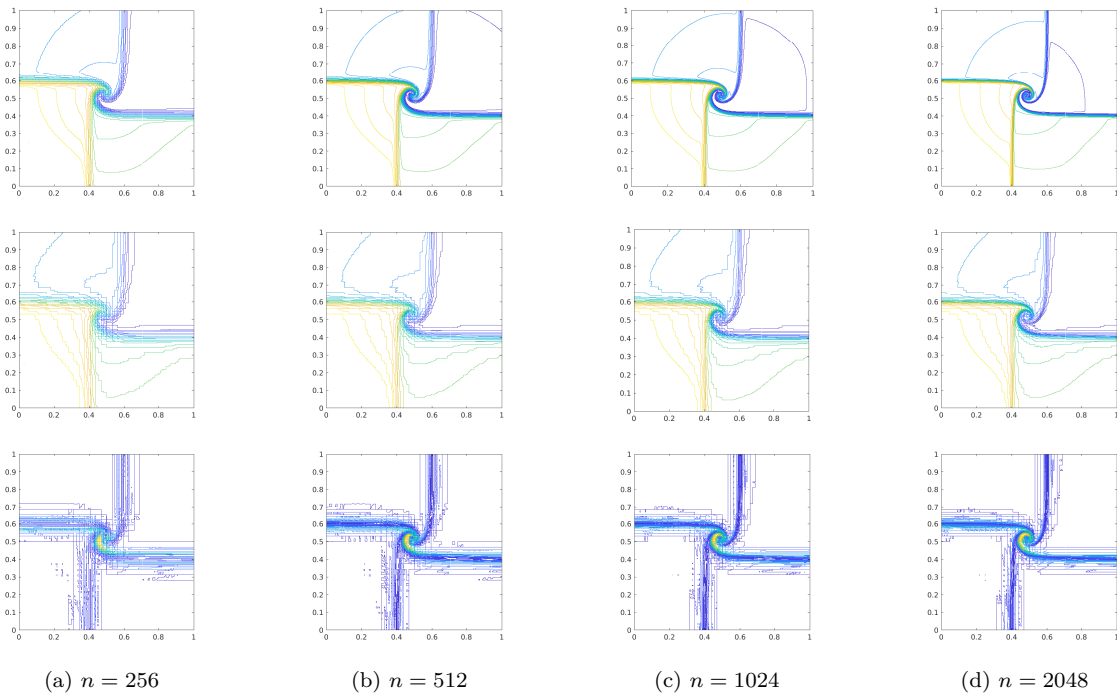


Figure 5.2: Example 5.1: the density contours obtained on meshes with $n \times n$ cells. From top to bottom: density (top); Cesáro averages of density (middle); the first variance of density (bottom).

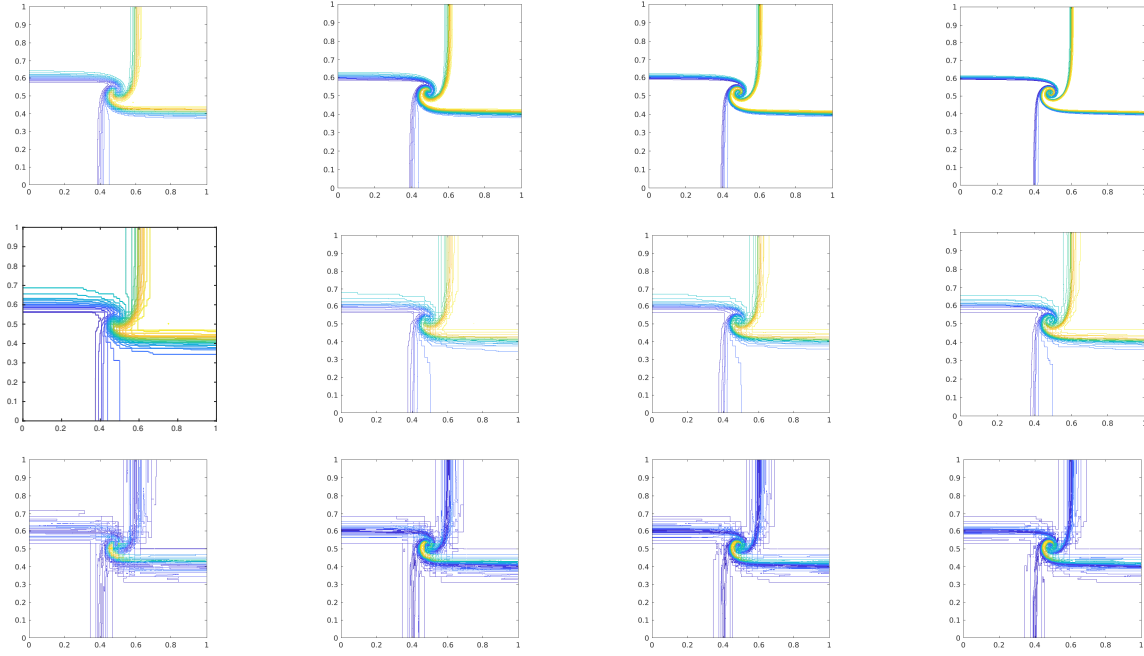
(a) $n = 256$ (b) $n = 512$ (c) $n = 1024$ (d) $n = 2048$

Figure 5.3: Example 5.1: the entropy contours obtained on meshes with $n \times n$ cells. From top to bottom: entropy (top); Cesáro averages of entropy (middle); the first variance of entropy (bottom).

Example 5.2 (Kelvin-Helmholtz problem). We consider a shear flow of three fluid layers with different densities. The initial data are given by

$$(\rho, u, v, p)(x, 0) = \begin{cases} (2, -0.5, 0, 2.5), & \text{if } I_1 < x_2 < I_2, \\ (1, 0.5, 0, 2.5), & \text{otherwise,} \end{cases}$$

where the interface profiles

$$I_j = I_j(\mathbf{x}) := J_j + \epsilon Y_j(\mathbf{x}), \quad j = 1, 2$$

are chosen to be small perturbations around the lower $J_1 = 0.25$ and the upper $J_2 = 0.75$ interfaces, respectively. Moreover,

$$Y_j = \sum_{m=1}^M a_j^m \cos(b_j^m + 2n\pi x_1), \quad j = 1, 2,$$

where $a_j^m \in [0, 1]$ and $b_j^m \in [-\pi, \pi]$, $j = 1, 2, m = 1, \dots, M$ are arbitrary, but fixed numbers. The coefficients a_j^m have been normalized such that $\sum_{m=1}^M a_j^m = 1$ to guarantee that $|I_j - J_j| < \epsilon$ for $j = 1, 2$. In the simulation we have $M = 10, \epsilon = 0.01, T = 2$ and $N = 2048$.

Figure 5.4 shows the errors E_1, E_2, E_3, E_4 of ρ, m_1, m_2, E, S obtained on different meshes. Tables 5.3, 5.4 present the errors of ρ, S , respectively. Moreover, Figures 5.5, 5.6 show the contours of ρ and S obtained on different meshes, respectively.

The numerical results show that the numerical solutions obtained by the finite volume method (2.13) seem to converge in the sense of L^1 . Though, the convergence rates of E_2, E_3, E_4 are much higher than that of E_1 .

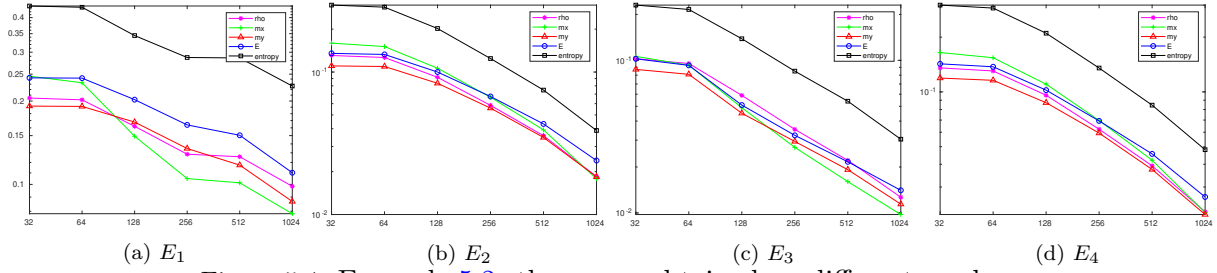


Figure 5.4: Example 5.2: the errors obtained on different meshes.

Table 5.3: Example 5.2: the errors and convergence rates for density.

n	E_1		E_2		E_3		E_4	
	error	order	error	order	error	order	error	order
32	0.2050	-	0.1307	-	0.1026	-	0.1355	-
64	0.2020	0.0215	0.1265	0.0468	0.0953	0.1052	0.1303	0.0561
128	0.1621	0.3175	0.0918	0.4620	0.0589	0.6939	0.0958	0.4437
256	0.1285	0.3345	0.0584	0.6542	0.0353	0.7393	0.0623	0.6202
512	0.1259	0.0303	0.0357	0.7072	0.0221	0.6750	0.0392	0.6682
1024	0.0984	0.3549	0.0185	0.9533	0.0127	0.8033	0.0219	0.8381

Table 5.4: Example 5.2: the errors and convergence rates for entropy.

n	E_1		E_2		E_3		E_4	
	error	order	error	order	error	order	error	order
32	0.4405	-	0.2950	-	0.2302	-	0.3000	-
64	0.4359	0.0152	0.2854	0.0479	0.2155	0.0952	0.2889	0.0543
128	0.3446	0.3392	0.2021	0.4980	0.1385	0.6375	0.2102	0.4593
256	0.2871	0.2631	0.1244	0.6998	0.0850	0.7052	0.1353	0.6355
512	0.2860	0.0055	0.0747	0.7356	0.0540	0.6544	0.0846	0.6779
1024	0.2265	0.3366	0.0389	0.9423	0.0304	0.8274	0.0481	0.8135

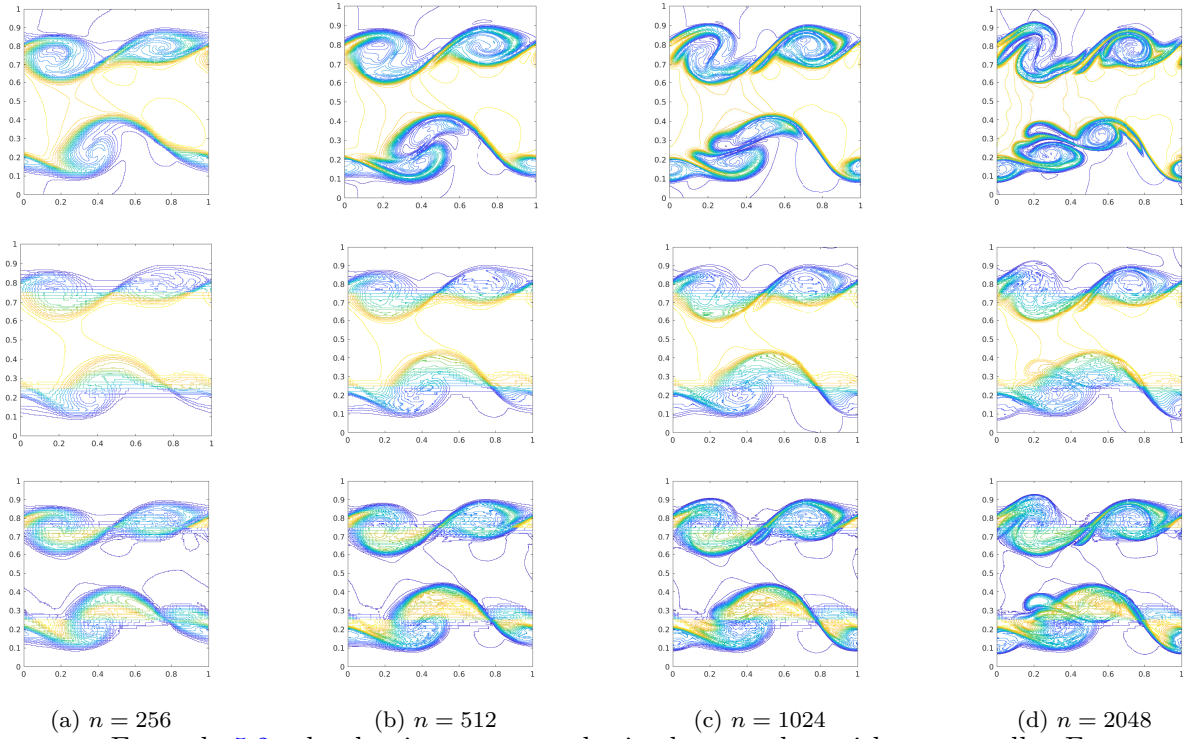


Figure 5.5: Example 5.2: the density contours obtained on meshes with $n \times n$ cells. From top to bottom: density (top); Cesáro averages of density (middle); the first variance of density (bottom).

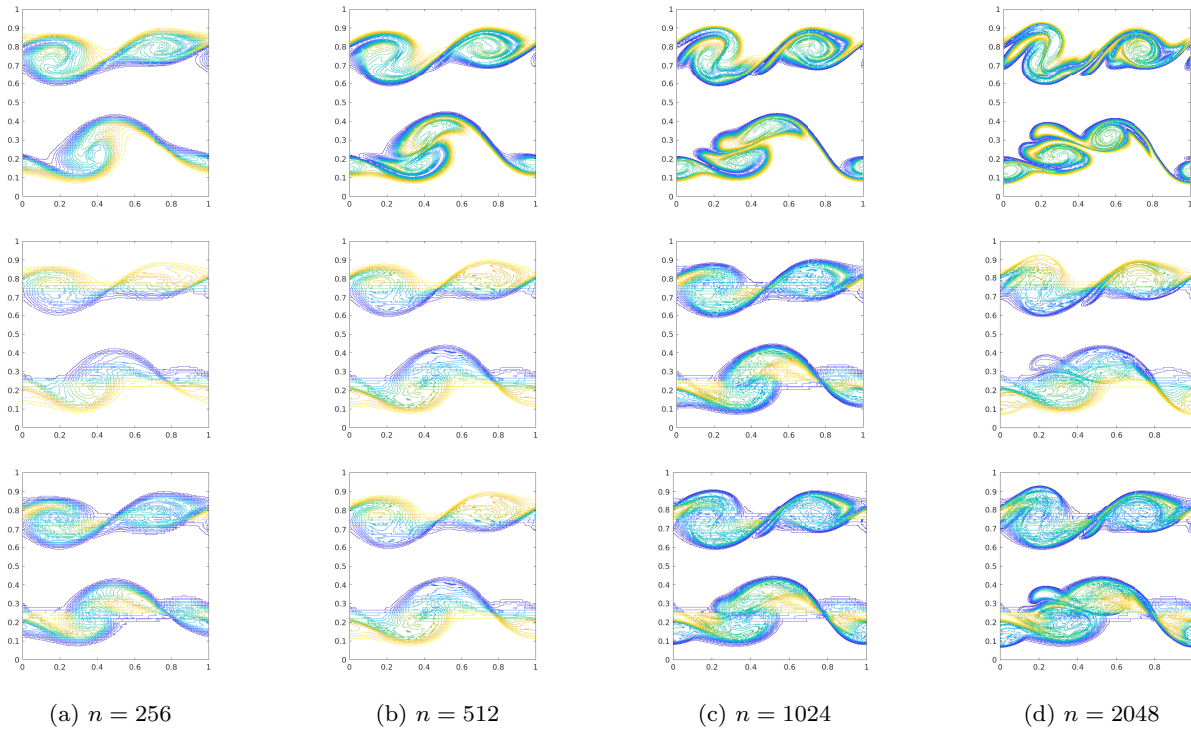


Figure 5.6: Example 5.2: the entropy contours obtained on meshes with $n \times n$ cells. From top to bottom: entropy (top); Cesáro averages of entropy (middle); the first variance of entropy (bottom).

Example 5.3 (Richtmyer-Meshkov problem). This example describes complex interactions of strong shocks with unstable interfaces. The initial data are given by

$$u_1 = 0, \quad u_2 = 0, \quad p(x, 0) = \begin{cases} 20, & \text{if } r < 0.1, \\ 1, & \text{otherwise,} \end{cases} \quad \rho(x, 0) = \begin{cases} 2, & \text{if } r < I(\mathbf{x}), \\ 1, & \text{otherwise,} \end{cases}$$

where $r = \sqrt{(x_1 - 0.5)^2 + (x_2 - 0.5)^2}$ and the radial interface $I(\mathbf{x}) = 0.25 + \epsilon Y(\mathbf{x})$ is perturbed by

$$Y(\mathbf{x}) = \sum_{m=1}^M a^m \cos(\phi + b^m),$$

with $\phi = \arccos((x_2 - 0.5)/r)$. The parameters a^m, b^m are arbitrary, but fixed numbers chosen such that $a^m \in [0, 1]$, $\sum_{m=1}^M a^m = 1$ and $b^m \in [-\pi, \pi]$, $m = 1, \dots, M$. In the simulation we set $\epsilon = 0.01, T = 4$ and $N = 2048$.

Figure 5.7 shows the errors E_1, E_2, E_3, E_4 of ρ, m_1, m_2, E, S obtained using different meshes $n = 32, \dots, 1024$, see also Tables 5.5, 5.6. Moreover, the contours of ρ and S are shown in Figures 5.8, 5.9, respectively.

The figures and tables clearly indicate only a weak converge of single simulations obtained by the finite volume method (2.13). Indeed, the numerical solutions do not converge strongly in L^1 -norm. On the other hand, the Cesàro average and the first variance of the numerical solutions, as well as the Wasserstein distance of the corresponding Dirac distributions converge strongly in L^1 -norm. These results again confirm our theoretical analysis on the convergence of the finite volume method (2.13). In the Richtmyer-Meshkov case the limiting solution is not a weak solution but a dissipative measure-valued solution.

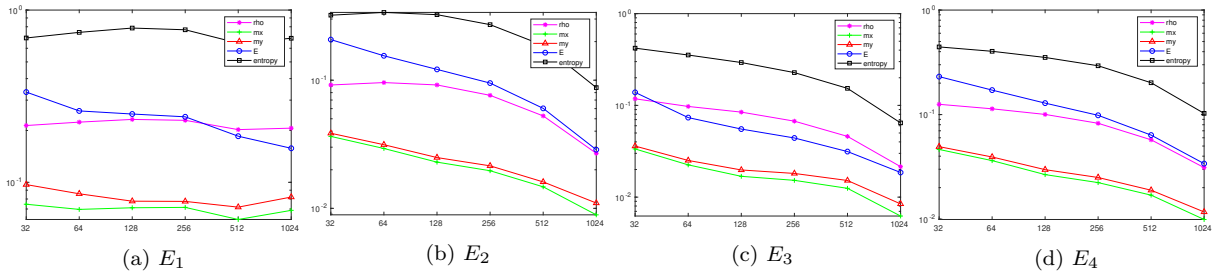


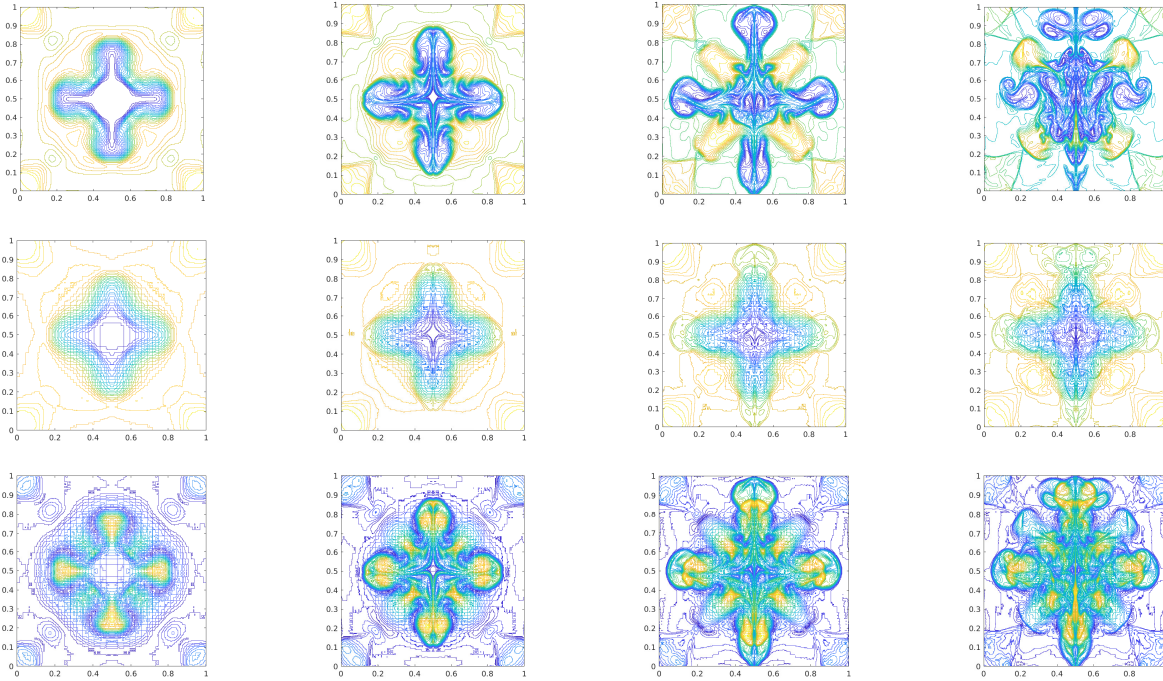
Figure 5.7: Example 5.3: the errors obtained on different meshes.

Table 5.5: Example 5.3: the errors and convergence rates for density.

n	E_1		E_2		E_3		E_4	
	error	order	error	order	error	order	error	order
32	0.2136	-	0.0917	-	0.1180	-	0.1254	-
64	0.2236	-0.0656	0.0958	-0.0626	0.0973	0.2774	0.1136	0.1433
128	0.2318	-0.0523	0.0918	0.0613	0.0844	0.2051	0.1004	0.1782
256	0.2290	0.0175	0.0762	0.2692	0.0673	0.3274	0.0826	0.2816
512	0.2023	0.1790	0.0526	0.5337	0.0459	0.5512	0.0574	0.5249
1024	0.2063	-0.0280	0.0269	0.9694	0.0215	1.0959	0.0311	0.8835

Table 5.6: Example 5.3: the errors and convergence rates for entropy.

n	E_1		E_2		E_3		E_4	
	error	order	error	order	error	order	error	order
32	0.6887	-	0.3215	-	0.4205	-	0.4440	-
64	0.7423	-0.1082	0.3378	-0.0716	0.3539	0.2487	0.4032	0.1391
128	0.7862	-0.0830	0.3246	0.0578	0.2931	0.2718	0.3521	0.1957
256	0.7684	0.0330	0.2713	0.2588	0.2277	0.3646	0.2932	0.2639
512	0.6425	0.2582	0.1869	0.5373	0.1533	0.5704	0.2017	0.5396
1024	0.6860	-0.0945	0.0876	1.0943	0.0645	1.2502	0.1027	0.9737



(a) $n = 256$

(b) $n = 512$

(c) $n = 1024$

(d) $n = 2048$

Figure 5.8: Example 5.3: the density contours obtained on meshes with $n \times n$ cells. From top to bottom: density (top); Cesàro averages of density (middle); the first variance of density (bottom).

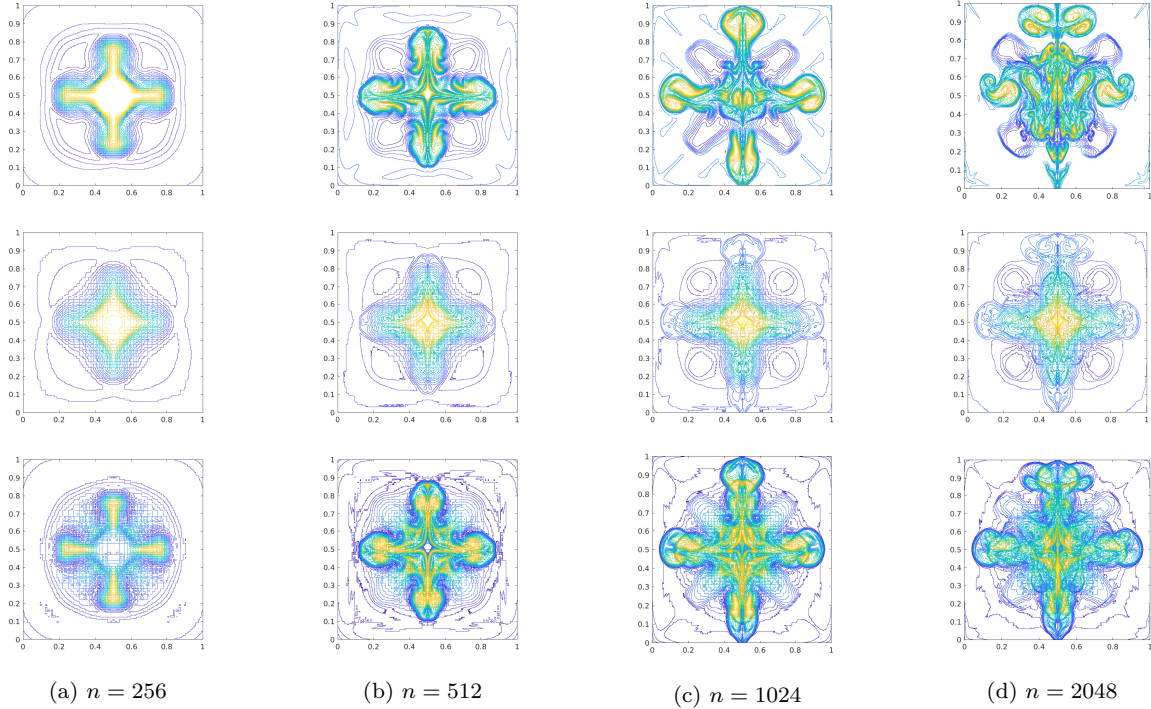


Figure 5.9: Example 5.3: the entropy contours obtained on meshes with $n \times n$ cells. From top to bottom: entropy (top); Cesáro averages of entropy (middle); the first variance of entropy (bottom).

6. Conclusions

We have shown the convergence of the Godunov finite volume method (2.13), which is based on the exact solution of a local Riemann problem for the complete compressible Euler system. Hereby we have only assumed that our numerical solutions belong to a physically non-degenerate region, i.e. we have a uniform lower bound on density and an upper bound on energy. The latter is equivalent to the existence of a uniform lower bound on entropy Hessian matrix, see Lemma B.4. Using the fact that the finite volume method (2.13) is entropy stable, the entropy inequality together with the explicit lower bound of the entropy Hessian matrix yield the weak BV estimate (3.9). Further, we have shown that the difference between the exact solution of the local Riemann problem and its initial data, i.e. numerical solution at time t_n , can be controlled by the jump of numerical solution itself. Consistency of the method is proved in Theorem 3.1. Weak convergence to a generalized solution, the dissipative measure-valued (DMV) solution, is showed in Theorem 4.1. Applying the novel tool of \mathcal{K} -convergence we obtained strong convergence to the expected value and first variance of a dissipative measure-valued solution, see Theorem 4.2. Theorem 4.3 summarizes the cases of strong convergence of numerical solutions of (2.13). The latter happens if the limit is a weak or C^1 solution to the Euler

system (2.1). In addition, applying the DMV-strong uniqueness principle [5] we also have strong convergence of our numerical solutions on the lifespan of the strong solution.

Numerical results for the spiral problem, the Kelvin-Helmholtz problem and the Richtmyer-Meshkov problem confirm results of theoretical analysis. In particular, we observe that for highly oscillatory limit, as is the case of the Richtmyer-Meshkov test, single numerical solutions do not converge strongly. On the other hand, we obtain the strong convergence of observable quantities, i.e. the expected values and first variances.

Although the Godunov finite volume method is one of the most classical schemes for hyperbolic conservation laws, its numerical analysis for multidimensional systems still remains open in general. The main goal of this paper was to fill this gap and illustrate the application of the recently developed concepts of generalized DMV solution and \mathcal{K} -convergence on an iconic example, the multidimensional Euler system. In future it will be interesting to extend the obtained results to general multidimensional hyperbolic conservation laws.

Acknowledgments

M.L. has been funded by the German Science Foundation (DFG) under the collaborative research projects TRR SFB 165 (Project A2) and TRR SFB 146 (Project C5). Y.Y. has been funded by Sino-German (CSC-DAAD) Postdoc Scholarship Program in 2020 - Project number 57531629.

References

- [1] J. M. Ball. A version of the fundamental theorem for young measures. In *PDEs and Continuum Models of Phase Transitions*, pages 207–215. Springer, 1989.
- [2] Y. Brenier, C. De Lellis, and L. Székelyhidi. Weak-strong uniqueness for measure-valued solutions. *Commun. Math. Phys.*, 305(2):351–361, 2011.
- [3] A. Bressan, G. Crasta, and B. Piccoli. *Well-Posedness of the Cauchy Problem for $n \times n$ Systems of Conservation Laws*. Memoirs of the American Mathematical Society, 2000.
- [4] A. Bressan and M. Lewicka. A uniqueness condition for hyperbolic systems of conservation laws. *Discrete Contin. Dyn. Syst.*, 6(3):673–682, 2000.
- [5] J. Březina and E. Feireisl. Measure-valued solutions to the complete Euler system. *J. Math. Soc. Japan*, 70(4):1227 – 1245, 2018.
- [6] T.H. Chen and C.W. Shu. Entropy stable high order discontinuous Galerkin methods with suitable quadrature rules for hyperbolic conservation laws. *J. Comput. Phys.*, 345(15):427–461, 2017.

- [7] E. Chiodaroli, C. De Lellis, and O. Kreml. Global ill-posedness of the isentropic system of gas dynamics. *Commun. Pure Appl. Math.*, 68(7):1157–1190, 2015.
- [8] C. De Lellis and L. Székelyhidi Jr. On admissibility criteria for weak solutions of the Euler equations. *Arch. Ration. Mech. Anal.*, 195(1):225–260, 2010.
- [9] S. Demoulini, D. M. A. Stuart, and A. E. Tzavaras. Weak–strong uniqueness of dissipative measure-valued solutions for polyconvex elastodynamics. *Arch. Ration. Mech. Anal.*, 205(3):927–961, 2012.
- [10] R.J. DiPerna. Measure-valued solutions to conservation laws. *Arch. Ration. Mech. Anal.*, 88(3):223–270, 1985.
- [11] R.J. DiPerna and A.J. Majda. Oscillations and concentrations in weak solutions of the incompressible fluid equations. *Commun. Math. Phys.*, 108(4):667–689, 1987.
- [12] E. Feireisl, P. Gwiazda, A. Świerczewska Gwiazda, and E. Wiedemann. Dissipative measure-valued solutions to the compressible Navier–Stokes system. *Calc. Var. Part. Diff. Eq.*, 55(6):141, 2016.
- [13] E. Feireisl, C. Klingenberg, O. Kreml, and S. Markfelder. On oscillatory solutions to the complete Euler system. *J. Differ. Equ.*, 269(2):1521–1543, 2020.
- [14] E. Feireisl, M. Lukáčová-Medvidřová, and H. Mizerová. A finite volume scheme for the Euler system inspired by the two velocities approach. *Numer. Math.*, 144(1):89–132, 2020.
- [15] E. Feireisl, M. Lukáčová-Medvidřová, and H. Mizerová. Convergence of finite volume schemes for the Euler Equations via dissipative measure-valued solutions. *Found. Comput. Math.*, 20(4):923–966, 2020.
- [16] E. Feireisl, M. Lukáčová-Medvidřová, and H. Mizerová. \mathcal{K} -convergence as a new tool in numerical analysis. *IMA J. Numer. Anal.*, 40(4):2227–2255, 2020.
- [17] E. Feireisl, M. Lukáčová-Medvidřová, H. Mizerová, and B. She. Convergence of a finite volume scheme for the compressible Navier-Stokes system. *ESAIM Math. Model. Numer. Anal.*, 53(6):1957–1979, 2019.
- [18] E. Feireisl, M. Lukáčová-Medvidřová, H. Mizerová, and B. She. *Numerical Analysis of Compressible Flows*. Springer, in print, 2021.
- [19] E. Feireisl, M. Lukáčová-Medvidřová, B. She, and Y. Wang. Computing oscillatory solutions of the Euler system via \mathcal{K} -convergence. *Math. Models Methods Appl. Sci.*, 2021.

- [20] M. Feistauer, J. Felcman, and I. Straškraba. *Mathematical and computational methods for compressible flow*. Numerical Mathematics and Scientific Computation. The Clarendon Press, Oxford University Press, Oxford, 2003.
- [21] U.S. Fjordholm, R. Käppeli, S. Mishra, and E. Tadmor. Construction of approximate entropy measure-valued solutions for hyperbolic systems of conservation laws. *Found. Comput. Math.*, 17(3):763–827, 2017.
- [22] U.S. Fjordholm, S. Mishra, and E. Tadmor. On the computation of measure-valued solutions. *Acta Numer.*, 25:567–679, 2016.
- [23] P. Gwiazda, A. Świerczewska-Gwiazda, and E. Wiedemann. Weak-strong uniqueness for measure-valued solutions of some compressible fluid models. *Nonlinearity*, 28(11):3873–3890, 2015.
- [24] A. Harten. On the symmetric form of systems of conservation laws with entropy. *J. Comput. Phys.*, 49(1):151–164, 1983.
- [25] A. Harten, P.D. Lax, and B. Van Leer. On upstream differencing and Godunov-type schemes for hyperbolic conservation laws. *SIAM Rev.*, 25(1):35–61, 1983.
- [26] D. Kröner and W. Zajaczkowski. Measure-valued solutions of the Euler equations for ideal compressible polytropic fluids. *Math. Methods Appl. Sci.*, 19(3):235–252, 1996.
- [27] S. Kružkov. First order quasilinear equations in several independent variables. *USSR Math. Sbornik*, 10(2):217–243, 1970.
- [28] J. Málek, J. Nečas, M. Rokyta, and M. Růžička. *Weak and Measure-valued Solutions to Evolutionary PDEs*. Chapman and Hall/CRC, 2019.
- [29] E. Tadmor. The numerical viscosity of entropy stable schemes for systems of conservation laws. I. *Math. Comp.*, 49(179):91–103, 1987.
- [30] E.F. Toro. *Riemann Solver and Numerical Methods for Fluid Dynamics, Third edition*. Springer-Verlag Berlin Heidelberg, 2009.

A. Lipschitz continuity of \mathbf{F}

The aim of this section is to give the estimates of $\| [(\mathbf{F}_1)_h] \|$, also denoted by $\| [F_h] \|$.

Lemma A.1. *It holds*

$$\{|\mathbf{u}|^2\} \leq (\| \{\mathbf{u}\} \| + \| [[\mathbf{u}]] \|)^2, \quad \{a^2\} \leq 2 \{a\}^2, \quad \{p\} \{\rho\}^{-1} \leq \frac{4}{\gamma} \{a\}^2, \quad (\text{A.1})$$

$$\{\rho|\mathbf{u}|^2\} \{\rho\}^{-1} \leq 2(\| \{\mathbf{u}\} \| + \| [[\mathbf{u}]] \|)^2, \quad \| \{\mathbf{m}\} \| \{\rho\}^{-1} \leq \| \{\mathbf{u}\} \| + \frac{1}{2} \| [[\mathbf{u}]] \|. \quad (\text{A.2})$$

Proof. If $f \geq 0$ then $|[[f]]| \leq \min(f_L, f_R) \leq 2\{f\}$. After some calculations we obtain

$$\{a^2\} = \{a\}^2 + \frac{1}{4} [[a]]^2 \leq 2\{a\}^2, \quad \{|\mathbf{u}|^2\} = \{\mathbf{u}\} \cdot \{\mathbf{u}\} + \frac{1}{4} [[\mathbf{u}]] \cdot [[\mathbf{u}]] \leq (\|\{\mathbf{u}\}\| + \|[[\mathbf{u}]] \|)^2.$$

Moreover, we obtain

$$\begin{aligned} \{p\} &= \left\{ \frac{p}{\rho} \cdot \rho \right\} = \left\{ \frac{p}{\rho} \right\} \{\rho\} + \frac{1}{4} \left[\left[\frac{p}{\rho} \right] \right] [[\rho]] \leq 2 \left\{ \frac{p}{\rho} \right\} \{\rho\} = \frac{2}{\gamma} \{a^2\} \{\rho\}, \\ \{\rho|\mathbf{u}|^2\} &= \{\rho\} \{|\mathbf{u}|^2\} + \frac{1}{4} [[\rho]] [[|\mathbf{u}|^2]] \leq 2\{\rho\} \{|\mathbf{u}|^2\}, \\ \|\{\mathbf{m}\}\| &= \|\{\rho\} \{\mathbf{u}\} + \frac{1}{4} [[\rho]] [[\mathbf{u}]]\| \leq \{\rho\} \|\{\mathbf{u}\}\| + \frac{1}{2} \{\rho\} \|[[\mathbf{u}]] \|, \end{aligned}$$

which concludes the proof. \square

Lemma A.2. *It holds*

$$\|[[\mathbf{u}]] \| \leq \{\rho\}^{-1} \|\{\mathbf{u}\}\| \cdot |[[\rho]] | + \{\rho\}^{-1} \|[[\mathbf{m}]] \|, \quad (\text{A.3})$$

$$|[[p]]| \lesssim (\|\{\mathbf{u}\}\| + \|[[\mathbf{u}]] \|)^2 \cdot |[[\rho]] | + (\|\{\mathbf{u}\}\| + \|[[\mathbf{u}]] \|) \cdot \|[[\mathbf{m}]] \| + |[[E]]|. \quad (\text{A.4})$$

Proof. Some manipulations give

$$[[\mathbf{m}]] = \{\rho\} [[\mathbf{u}]] + [[\rho]] \{\mathbf{u}\},$$

which implies

$$\|[[\mathbf{u}]] \| = \left\| \frac{[[\mathbf{m}]] - [[\rho]] \{\mathbf{u}\}}{\{\rho\}} \right\| \leq \{\rho\}^{-1} \|\{\mathbf{u}\}\| \cdot |[[\rho]] | + \{\rho\}^{-1} \|[[\mathbf{m}]] \|.$$

On the other hand, we have

$$\left[\left[\frac{|\mathbf{m}|^2}{\rho} \cdot \rho \right] \right] = [[|\mathbf{m}|^2]] = \{\mathbf{m}\} \cdot [[\mathbf{m}]] = \left\{ \frac{|\mathbf{m}|^2}{\rho} \right\} \cdot [[\rho]] + \left[\left[\frac{|\mathbf{m}|^2}{\rho} \right] \right] \cdot \{\rho\},$$

which gives

$$\left| \left[\left[\frac{|\mathbf{m}|^2}{\rho} \right] \right] \right| \leq \{\rho\}^{-1} \left\{ \frac{|\mathbf{m}|^2}{\rho} \right\} \cdot |[[\rho]] | + \{\rho\}^{-1} \|\{\mathbf{m}\}\| \cdot \|[[\mathbf{m}]] \|.$$

Consequently, we obtain

$$\begin{aligned} |[[p]]| &= (\gamma - 1) \left| \left[\left[E - \frac{|\mathbf{m}|^2}{2\rho} \right] \right] \right| \leq (\gamma - 1) |[[E]]| + \frac{\gamma - 1}{2} \left| \left[\left[\frac{|\mathbf{m}|^2}{\rho} \right] \right] \right| \\ &\leq \frac{\gamma - 1}{2} \{\rho\}^{-1} \left\{ \frac{|\mathbf{m}|^2}{\rho} \right\} \cdot |[[\rho]] | + \frac{\gamma - 1}{2} \{\rho\}^{-1} \|\{\mathbf{m}\}\| \cdot \|[[\mathbf{m}]] \| + (\gamma - 1) |[[E]]|, \end{aligned}$$

which concludes the proof. \square

Lemma A.3. *It holds*

$$\begin{aligned}
\left| \left[\left[F^{(1)} \right] \right] \right| &\leq \| [\mathbf{m}] \|, \\
\left| \left[\left[F^{(2)} \right] \right] \right| &\lesssim (\| \{\mathbf{u}\} \| + \| [\mathbf{u}] \|^2) \cdot |[\rho]| + (\| \{\mathbf{u}\} \| + \| [\mathbf{u}] \|) \cdot \| [\mathbf{m}] \| + | [E] |, \\
\left| \left[\left[F^{(3)} \right] \right] \right| &\lesssim (\| \{\mathbf{u}\} \| + \| [\mathbf{u}] \|^2) \cdot |[\rho]| + (\| \{\mathbf{u}\} \| + \| [\mathbf{u}] \|) \cdot \| [\mathbf{m}] \|, \\
\left| \left[\left[F^{(4)} \right] \right] \right| &\lesssim (\| \{\mathbf{u}\} \| + \| [\mathbf{u}] \|^2) \cdot |[\rho]| + (\| \{\mathbf{u}\} \| + \| [\mathbf{u}] \|) \cdot \| [\mathbf{m}] \|, \\
\left| \left[\left[F^{(5)} \right] \right] \right| &\lesssim \left((\| \{\mathbf{u}\} \| + \| [\mathbf{u}] \|^2) + \{a\}^2 \right) \| \{\mathbf{u}\} \| \cdot |[\rho]| + (\| \{\mathbf{u}\} \| + \| [\mathbf{u}] \|^2) \cdot \| [\mathbf{m}] \| + \| \{\mathbf{u}\} \| \cdot | [E] |.
\end{aligned}$$

Proof. Some calculations give

$$\begin{aligned}
\left| \left[\left[F^{(1)} \right] \right] \right| &= | [\rho u] | \leq \| [\mathbf{m}] \|, \\
\left| \left[\left[F^{(2)} \right] \right] \right| &= | [\rho u^2 + p] | \leq \{u^2\} \cdot |[\rho]| + 2 \{\rho\} \cdot | \{u\} | \cdot | [u] | + | [p] | \\
&\leq \{|\mathbf{u}|^2\} \cdot |[\rho]| + 2 \{\rho\} \cdot \| \{\mathbf{u}\} \| \cdot \| [\mathbf{u}] \| + | [p] |, \\
\left| \left[\left[F^{(3)} \right] \right] \right| &= | [\rho uv] | \leq | \{uv\} | \cdot |[\rho]| + \{\rho\} \cdot | \{u\} | \cdot | [v] | + \{\rho\} \cdot | \{v\} | \cdot | [u] | \\
&\leq \{|\mathbf{u}|^2\} \cdot |[\rho]| + 2 \{\rho\} \cdot \| \{\mathbf{u}\} \| \cdot \| [\mathbf{u}] \|, \\
\left| \left[\left[F^{(4)} \right] \right] \right| &= | [\rho uw] | \leq | \{uw\} | \cdot |[\rho]| + \{\rho\} \cdot | \{u\} | \cdot | [w] | + \{\rho\} \cdot | \{w\} | \cdot | [u] | \\
&\leq \{|\mathbf{u}|^2\} \cdot |[\rho]| + 2 \{\rho\} \cdot \| \{\mathbf{u}\} \| \cdot \| [\mathbf{u}] \|
\end{aligned}$$

and

$$\begin{aligned}
\left| \left[\left[F^{(5)} \right] \right] \right| &= | [u(E + p)] | \leq \{E + p\} \cdot | [u] | + | \{u\} | \cdot | [E] | + | \{u\} | \cdot | [p] | \\
&\leq \{E + p\} \cdot \| [\mathbf{u}] \| + \| \{\mathbf{u}\} \| \cdot | [E] | + \| \{\mathbf{u}\} \| \cdot | [p] |.
\end{aligned}$$

Combining Lemma A.1 and Lemma A.2 concludes the proof. \square

B. Lower bound of the entropy Hessian matrix

In this section we give the lower bound of entropy Hessian matrix $\frac{d^2\eta}{d\mathbf{U}^2}$ for $d = 3$. Harten [24] has already given the explicit expression of $\frac{d^2\eta}{d\mathbf{U}^2}$ in two-dimensional case. Analogously, we can obtain its three-dimensional explicit expression with $\eta = -\rho\chi(S)$, $\chi \in C^2(\mathbb{R})$

$$\frac{d^2\eta}{d\mathbf{U}^2} = \frac{d\boldsymbol{\nu}}{d\mathbf{U}} = \left(\frac{\gamma - 1}{p} \right)^2 \rho\chi'(S) \cdot \mathbf{D},$$

where

$$\begin{aligned}
\mathbf{D}^{(1)} &:= \begin{pmatrix} \frac{|\mathbf{u}|^4}{4} + \frac{a_*^4}{\gamma} - R\left(\frac{|\mathbf{u}|^2}{2} - a_*^2\right)^2 \\ -u\left(\frac{|\mathbf{u}|^2}{2}(1-R) + Ra_*^2\right) \\ -v\left(\frac{|\mathbf{u}|^2}{2}(1-R) + Ra_*^2\right) \\ -w\left(\frac{|\mathbf{u}|^2}{2}(1-R) + Ra_*^2\right) \\ \frac{|\mathbf{u}|^2}{2}(1-R) - a_*^2\left(\frac{1}{\gamma} - R\right) \end{pmatrix}, \quad a_*^2 = \frac{\gamma}{\gamma-1} \cdot \frac{p}{\rho}, \quad R = \frac{\chi''(S)}{\chi'(S)}, \\
\mathbf{D}^{(2)} &:= \begin{pmatrix} -u\left(\frac{|\mathbf{u}|^2}{2}(1-R) + Ra_*^2\right) \\ u^2(1-R) + a_*^2/\gamma \\ uv(1-R) \\ uw(1-R) \\ -u(1-R) \end{pmatrix}, \quad \mathbf{D}^{(3)} := \begin{pmatrix} -v\left(\frac{|\mathbf{u}|^2}{2}(1-R) + Ra_*^2\right) \\ uv(1-R) \\ v^2(1-R) + a_*^2/\gamma \\ vw(1-R) \\ -v(1-R) \end{pmatrix}, \\
\mathbf{D}^{(4)} &:= \begin{pmatrix} -w\left(\frac{|\mathbf{u}|^2}{2}(1-R) + Ra_*^2\right) \\ uw(1-R) \\ vw(1-R) \\ w^2(1-R) + a_*^2/\gamma \\ -w(1-R) \end{pmatrix}, \quad \mathbf{D}^{(5)} := \begin{pmatrix} \frac{|\mathbf{u}|^2}{2}(1-R) - a_*^2\left(\frac{1}{\gamma} - R\right) \\ -u(1-R) \\ -v(1-R) \\ -w(1-R) \\ 1-R \end{pmatrix}.
\end{aligned}$$

Moreover, the symmetric matrix \mathbf{D} is positive definite if and only if $R < 1/\gamma$.

Consider the special case $\eta = -\rho S/(\gamma - 1)$, i.e., $\chi'(S) = 1/(\gamma - 1)$ and $\chi''(S) = 0$. After some calculations we obtain the characteristic function $f(\lambda)$ of the matrix \mathbf{D}

$$f(\lambda) = \left(\lambda - \frac{a^2}{\gamma}\right)^2 \cdot g(\lambda),$$

where

$$\begin{aligned}
g(\lambda) &= \lambda^3 - \frac{1}{4\gamma} \left(4a^4 + 4a^2 + \gamma(|\mathbf{u}|^2 + 2)^2\right) \lambda^2 \\
&\quad + \frac{a^2}{4\gamma^2} \left(4a^4 - 4a^2 + \gamma[4(|\mathbf{u}|^2 + 1)a^2 + (|\mathbf{u}|^2 + 2)^2]\right) \lambda - \frac{a^6(\gamma - 1)}{\gamma^3}.
\end{aligned}$$

Taking derivation of $g(\lambda)$ gives

$$\begin{aligned}
g'(\lambda) &= 3\lambda^2 - \frac{1}{2\gamma} \left(4a^4 + 4a^2 + \gamma(|\mathbf{u}|^2 + 2)^2\right) \lambda \\
&\quad + \frac{a^2}{4\gamma^2} \left(4a^4 - 4a^2 + \gamma[4(|\mathbf{u}|^2 + 1)a^2 + (|\mathbf{u}|^2 + 2)^2]\right).
\end{aligned}$$

Denote the roots of $g(\lambda) = 0$ by $\lambda_1, \lambda_2, \lambda_3$ with $\lambda_1 < \lambda_2 < \lambda_3$, the roots of $g'(\lambda) = 0$ by λ_1^* and λ_2^* with

$$\lambda_1^* \leq \frac{1}{12\gamma} (4a^4 + 4a^2 + \gamma(|\mathbf{u}|^2 + 2)^2) \leq \lambda_2^*. \quad (\text{B.1})$$

As known, $\frac{d^2\eta}{dU^2}$ is positive definite [24], which implies

$$0 < \lambda_1 \leq \lambda_1^* \leq \lambda_2 \leq \lambda_2^* \leq \lambda_3. \quad (\text{B.2})$$

Lemma B.1. *It holds*

$$\lambda_1 \leq \frac{a^2}{\gamma}(\gamma - 1)^{1/3} < \lambda_2. \quad (\text{B.3})$$

Remark B.1. *With the help of (B.1) and the fact*

$$\begin{cases} g(\lambda) < 0, & \text{if } \lambda \in (0, \lambda_1); & g(\lambda) > 0, & \text{if } \lambda \in (\lambda_1, \lambda_2); \\ g(\lambda) < 0, & \text{if } \lambda \in (\lambda_2, \lambda_3); & g(\lambda) > 0, & \text{if } \lambda \in (\lambda_3, 0); \end{cases}$$

we will prove Lemma B.1 by showing

$$g\left(\frac{a^2}{\gamma}(\gamma - 1)^{1/3}\right) \geq 0, \quad \frac{a^2}{\gamma}(\gamma - 1)^{1/3} < \frac{1}{12\gamma} (4a^4 + 4a^2 + \gamma(|\mathbf{u}|^2 + 2)^2) \leq \lambda_2^* \leq \lambda_3.$$

Proof. Denote $(\gamma - 1)^{1/3}$ by γ_* , i.e., $\gamma = \gamma_*^3 + 1$. Then $\gamma \in (1, 2]$ implies

$$\gamma_* \in (0, 1]. \quad (\text{B.4})$$

It is easy to show that

$$\begin{aligned} g\left(\frac{a^2\gamma_*}{\gamma}\right) &= \frac{a^4\gamma_*}{4\gamma^3} \left((1 - \gamma_*) \cdot (\gamma|\mathbf{u}|^4 + 4\gamma|\mathbf{u}|^2) + 4\gamma a^2|\mathbf{u}|^2 + 4(1 - \gamma_*) \cdot (a^4 - \gamma_*(1 + \gamma_*)a^2 + \gamma) \right) \\ &\geq \frac{a^4\gamma_*(1 - \gamma_*)}{\gamma^3} \left(a^4 - \gamma_*(1 + \gamma_*)a^2 + \gamma \right). \end{aligned}$$

Since

$$\Delta = (\gamma_*(1 + \gamma_*))^2 - 4\gamma = \gamma_*^2(1 - \gamma_*)^2 - 4 < 0,$$

we have $g\left(\frac{a^2\gamma_*}{\gamma}\right) \geq 0$.

On the other hand, we have

$$\frac{4a^4 + 4a^2 + \gamma(|\mathbf{u}|^2 + 2)^2}{12\gamma} - \frac{a^2}{\gamma}\gamma_* \geq \frac{4a^4 + 4a^2 + 4\gamma - a^2\gamma_*}{12\gamma} = \frac{1}{3\gamma} (a^4 + (1 - 3\gamma_*)a^2 + \gamma).$$

Hence,

$$\Delta = (1 - 3\gamma_*)^2 - 4\gamma = -3 - 6\gamma_* + 9\gamma_*^2 - 4\gamma_*^3 = -3(1 - \gamma_*^2) - 6(\gamma_* - \gamma_*^2) - 4\gamma_*^3 \leq 0,$$

which concludes the proof. \square

Lemma B.2. *It holds*

$$\lambda_1 \geq \frac{a^2(\gamma-1)}{\gamma} \min \left(\frac{a^2}{\gamma(|\mathbf{u}|^2+2)^2}, \frac{1}{4(a^2+1)}, \frac{1}{4\gamma(|\mathbf{u}|^2+1)} \right). \quad (\text{B.5})$$

Proof. Let $\lambda = \frac{a^2}{\gamma}x$. From Lemma B.1 we know that the lower boundary of λ_1 can only be found within $0 < x \leq 1$. With the definition of $g(\lambda)$ the following decomposition gives

$$\begin{aligned} g\left(\frac{a^2}{\gamma}x\right) &= \left(\frac{a^6x^3}{\gamma^3} - \frac{a^6(\gamma-1)}{4\gamma^3}\right) + \frac{a^4}{4\gamma^3} \left(-3a^2(\gamma-1) - 8a^2x \right. \\ &\quad \left. + \gamma(|\mathbf{u}|^2+2)^2x(1-x) + 4a^2(a^2+1)x(1-x) + 4\gamma a^2(|\mathbf{u}|^2+1)x\right) \\ &< \left(\frac{a^6x^3}{\gamma^3} - \frac{a^6(\gamma-1)}{4\gamma^3}\right) + \frac{a^4}{4\gamma^3} \left(\left[\gamma(|\mathbf{u}|^2+2)^2x(1-x) - a^2(\gamma-1)\right] \right. \\ &\quad \left. + \left[4a^2(a^2+1)x(1-x) - a^2(\gamma-1)\right] + \left[4\gamma a^2(|\mathbf{u}|^2+1)x - a^2(\gamma-1)\right]\right) \\ &< \left(\frac{a^6x^3}{\gamma^3} - \frac{a^6(\gamma-1)}{4\gamma^3}\right) + \frac{a^4}{4\gamma^3} \left(\left[\gamma(|\mathbf{u}|^2+2)^2x - a^2(\gamma-1)\right] \right. \\ &\quad \left. + \left[4a^2(a^2+1)x - a^2(\gamma-1)\right] + \left[4\gamma a^2(|\mathbf{u}|^2+1)x - a^2(\gamma-1)\right]\right), \end{aligned}$$

where the first inequality holds since $-8a^2x < 0$, and the second inequality due to $1-x < 1$. Hence, if x satisfies

$$x \leq \min \left(\left(\frac{\gamma-1}{4}\right)^{1/3}, \frac{a^2(\gamma-1)}{\gamma(u^2+2)^2}, \frac{\gamma-1}{4(a^2+1)}, \frac{\gamma-1}{4\gamma(u^2+1)} \right),$$

then $g(\lambda) < 0$. This concludes the proof since $\left(\frac{\gamma-1}{4}\right)^{1/3} > \frac{\gamma-1}{4}$. \square

Summarizing, we have the estimate for the smallest eigenvalue of the entropy Hessian matrix $\frac{d^2\eta}{d\mathbf{U}^2}$.

Lemma B.3. *It holds*

$$\min \left(\lambda \left(\frac{d^2\eta}{d\mathbf{U}^2} \right) \right) \in \left[\frac{(\gamma-1)^2}{p} \min \left(\frac{a^2}{\gamma(|\mathbf{u}|^2+2)^2}, \frac{1}{4(a^2+1)}, \frac{1}{4\gamma(|\mathbf{u}|^2+1)} \right), \frac{(\gamma-1)^{4/3}}{p} \right], \quad (\text{B.6})$$

where $\lambda \left(\frac{d^2\eta}{d\mathbf{U}^2} \right)$ represents the eigenvalue of matrix $\frac{d^2\eta}{d\mathbf{U}^2}$ and $\eta = -\frac{\rho S}{\gamma-1}$.

Specially, $\underline{\cdot}$, $\bar{\cdot}$ stand here for the infimum and supremum, respectively. For example,

$$\underline{\rho} = \inf(\rho), \quad \bar{E} = \sup(E), \quad \underline{\eta} = \inf \left(\min \left(\lambda \left(\frac{d^2\eta}{d\mathbf{U}^2} \right) \right) \right), \quad (\text{B.7})$$

where $\lambda \left(\frac{d^2\eta}{d\mathbf{U}^2} \right)$ represents the eigenvalue of matrix $\frac{d^2\eta}{d\mathbf{U}^2}$.

Lemma B.4. *The following is equivalent:*

- (i) $\underline{\rho} > 0, \bar{E} < \infty$ for a.e. $(t, \mathbf{x}) \in (0, T) \times \Omega$;
- (ii) $\underline{\eta} > 0$ for a.e. $(t, \mathbf{x}) \in (0, T) \times \Omega$.

Proof. Step 1: Suppose that (i) holds. Combining Lemma 3.1 and Lemma B.3 we have

$$\underline{\eta} \geq \frac{(\gamma - 1)^2}{\bar{p}} \min \left(\frac{\underline{a}^2}{\gamma(\bar{u}^2 + 2)^2}, \frac{1}{4(\bar{a}^2 + 1)}, \frac{1}{4\gamma(\bar{u}^2 + 1)} \right) > 0,$$

where $\bar{a} := \sqrt{\frac{\gamma \bar{p}}{\underline{\rho}}}, \underline{a} := \sqrt{\frac{\gamma \underline{p}}{\bar{\rho}}}$ and $\bar{\rho}, \underline{p}, \bar{p}, \bar{u}$ are defined in the proof of Lemma 3.1.

Step 2: Let (ii) hold. From (B.6) we obtain

$$\bar{p} < \infty. \tag{B.8}$$

In the following, with the relationship

$$\min \left(\lambda \left(\frac{d^2 \eta}{dU^2} \right) \right) = \lambda_1 \cdot \frac{\gamma(\gamma - 1)}{pa^2} = \lambda_1 \cdot \frac{\gamma^2(\gamma - 1)}{\rho a^4} \tag{B.9}$$

we show (i) by contradiction.

- $\bar{\rho} < \infty$.

Let \mathbf{u}, a fixed. It is the fact that $g(\lambda)$ only depends on $a^2, |\mathbf{u}|^2$, which implies λ_1 fixed. Hence, we can derive $\bar{\rho} < \infty$ from (B.9).

- $\bar{u} < \infty$.

Let a, p fixed. With $\underline{\eta} > 0$ we obtain $\underline{\lambda}_1 > 0$. Letting $|\mathbf{u}| \rightarrow \infty$ gives the behavior of $g(\lambda)$

$$g(\lambda) = \frac{(|\mathbf{u}|^2 + 2)^2}{4\gamma} \cdot \lambda \cdot (a^2 - \gamma\lambda) + \frac{a^2(|\mathbf{u}|^2 + 1)}{4\gamma} \lambda.$$

Combining $\lambda_1 > \underline{\lambda}_1 > 0$ implies $g(\lambda_1) \rightarrow \infty$ or $g(\lambda_1) \rightarrow -\infty$, which is a contradiction with $g(\lambda_1) = 0$.

- $\underline{\rho} > 0$.

Let $\mathbf{u} \neq 0, p$ fixed. With $\underline{\eta} > 0$ we obtain $\frac{\lambda_1}{a^2} > 0$. Call back that

$$g \left(\frac{a^2}{\gamma} x \right) = \frac{a^6}{\gamma^3} \left((x - 1)^2(x + 1) + \gamma[(|\mathbf{u}|^2 + 1)x - 1] \right) + \frac{a^4}{4\gamma^2} \gamma (|\mathbf{u}|^2 + 2)^2 x(1 - x) + \frac{a^8}{\gamma^3} x(1 - x).$$

We let $\lambda_1 = \frac{a^2}{\gamma} x$, which implies that x satisfies $\bar{x} > 0$ and $\bar{x} \leq 1$. Passing to the limit $\rho \rightarrow 0$, i.e. $a^2 \rightarrow \infty$, we obtain $g(\lambda_1) \rightarrow \infty$, which is a contradiction.

Consequently, it holds $E \leq \frac{1}{2} \bar{\rho} \bar{u}^2 + \frac{1}{\gamma - 1} \bar{p}$, which concludes the proof. \square